Journal Code	Article ID	Dispatch: 26-JUN-20	CE:
JBMB	34681	No. of Pages: 23	ME:

Received: 17 February 2020 | Revised: 4 June 2020 | Accepted: 16 June 2020

DOI: 10.1002/jbm.b.34681

REVIEW ARTICLE

Foam-in-vein: A review of rheological properties and characterization methods for optimization of sclerosing foams

Alireza Meghdadi[1] | Stephen A. Jones[2] | Venisha A. Patel[2] | Andrew L. Lewis[2] | Timothy M. Millar[3] | Dario Carugo[1,4]

[1]Faculty of Engineering and Physical Sciences, University of Southampton, Southampton, UK

[2]Biocompatibles UK Ltd, Camberley, UK

[3]Faculty of Medicine, University of Southampton, Southampton, UK

[4]Institute for Life Sciences (IfLS), University of Southampton, Southampton, UK

Correspondence
Dario Carugo, Faculty of Engineering and Physical Sciences, University of Southampton, Southampton, UK.
Email: d.carugo@soton.ac.uk

Funding information
University of Southampton; Engineering and Physical Sciences Research Council

Abstract

Varicose veins are chronic venous defects that affect >20% of the population in developed countries. Among potential treatments, sclerotherapy is one of the most commonly used. It involves endovenous injection of a surfactant solution (or foam) in varicose veins, inducing damage to the endothelial layer and subsequent vessel sclerosis. Treatments have proven to be effective in the short-term, however recurrence is reported at rates of up to 64% 5-year post-treatment. Thus, once diagnosed with varicosities there is a high probability of a permanently reduced quality of life. Recently, foam sclerotherapy has become increasingly popular over its liquid counterpart, since foams can treat larger and longer varicosities more effectively, they can be imaged using ultrasound, and require lower amounts of sclerosing agent. In order to minimize recurrence rates however, an investigation of current treatment methods should lead to more effective and long-lasting effects. The literature is populated with studies aimed at characterizing the fundamental physics of aqueous foams; nevertheless, there is a significant need for appropriate product development platforms. Despite successfully capturing the microstructural evolution of aqueous foams, the complexity of current models renders them inadequate for pharmaceutical development. This review article will focus on the physics of foams and the attempts at optimizing them for sclerotherapy. This takes the form of a discussion of the most recent numerical and experimental models, as well as an overview of clinically relevant parameters. This holistic approach could contribute to better foam characterization methods that patients may eventually derive long term benefit from.

KEYWORDS

aqueous foams, foam sclerotherapy, sclerotherapy, vascular therapies

1 | INTRODUCTION

The mechanical work performed by the calf muscles is the primary driver for blood return in the circulation. The heart pumps blood throughout the body via vascular conduits, that is, arteries (carriers of oxygenated blood) and veins (carriers of deoxygenated blood). For deoxygenated blood to reach the heart from the lower limbs, veins of the lower extremities need to do work against hydrostatic pressure caused by gravity. Given the lack of active mechanical work provided by the vein's valves, venous return relies almost entirely on external

mechanical stimuli such as muscle contraction, although physiological venous valves in the lower limb veins prohibit the backflow of blood (Figure 1). If and when blood leaks through these valves, over time the vessel may dilate resulting in incompetent valves (Gloviczki et al., 2011; Oklu et al., 2012). Consequently, these vessels are prone to insufficiencies in adults that can arise due to factors such as age, pregnancy, lack of exercise, and obesity. Once developed, these insufficiencies manifest into varicose veins—regions of twisted and dilated vessels ineffective at venous blood return back to the heart (Eckmann, 2009).

A common minimally invasive treatment is sclerotherapy, involving the injection of a surfactant into the vessel, causing lysis of venous endothelium and resulting in sclerosis of the varicose vein (Gloviczki et al., 2011). Although an effective treatment, sclerotherapy does not eliminate varicosities completely. In fact varicosities may reoccur in up to 64% of cases after 5 years (Zhang & Melander, 2014). More invasive methods such as venous stripping reduce the chances of recurrence (Jones, Braithwaite, Selwyn, Cooke, & Earnshaw, 1996; Van Rij, Jones, Hill, & Jiang, 2004). Thus, it is evident that non-invasive treatment options such as sclerotherapy need to be optimized. Some recent efforts have been made to optimize sclerosing foams in vitro (Bai et al., 2018; Critello, Fiorillo, & Matula, 2017; Wong, Chen, Connor, Behnia, & Parsi, 2015); however, they lack clinically relevant parameters that can correlate physical characteristics of foams with clinical outcomes of sclerotherapy. Other studies have instead defined new parameters that could directly reflect the performance of sclerosing foams (Bottaro et al., 2019; Carugo et al., 2013).

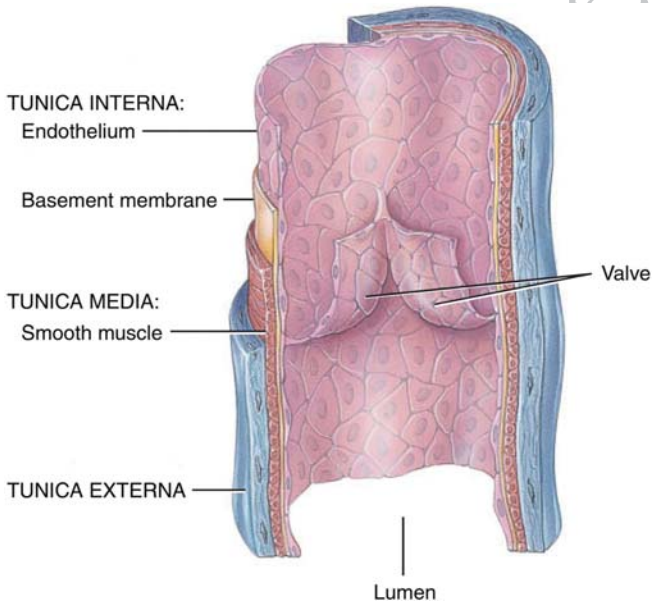

FIGURE 1 Anatomy of a vein valve. Healthy venous valves point toward the hearth and prevent blood from pooling inside the veins (Reprinted from Tortora et al., Copyright [2014], Gerard J. Tortora, L.L.C., Bryan Derrickson, John Wiley & Sons, Inc. All rights reserved, with permission from Wiley)

Sclerosants are injected as foams in order to maximize contact with the vessel wall. In order to optimize sclerotherapy, it is not only important to understand the underlying physical phenomena occurring in aqueous foams, but to identify clinically applicable metrics that correlate with therapeutic outcomes. This demands an in-depth knowledge of current physical models describing foam behavior. To this end, the following details a review of current literature discussing all aspects of foam behavior, ranging from microscopic phenomena to its flow behavior, and recent advancements in foam sclerotherapy and its physical characteristics.

2 | VARICOSE VEINS

Veins are the main carriers of deoxygenated blood in the body and also serve as functional blood reservoirs. They contain one-way bicuspid valves pointing toward deep veins and the heart, which prevent backflow of blood. Muscle contraction in the lower limbs can aid the flow of blood toward the heart. A number of circumstances are known to cause varicosities. For instance, mechanical stress as a consequence of pregnancy or prolonged periods of standing and ageing have been associated with varicose veins (Tortora & Derrickson, 2014). The growing uterus during pregnancy increases external pressure on lower limb veins that causes a decrease in venous blood return; this in turn results in pooling of blood (i.e., venous reflux) and increased venous pressure (i.e., venous hypertension). Standing still also raises venous hydrostatic pressure, due to hydrostatic effects and the absence of muscle contraction (Tortora & Derrickson, 2014; Whiteley, 2011; Zhang & Melander, 2014). Beebe-Dimmer et al. explores the effect of various epidemiological factors such as occupation, age, gender and diet on prevalence rates of chronic venous diseases (Beebe-Dimmer, Pfeifer, Engle, & Schottenfeld, 2005).

Under normal conditions, peripheral venous pressure is between 4 and 6 mmHg in lying adults while standing still can increase venous pressure to around 90 mmHg compared to 20 mmHg in walking adults (Guyton & Hall, 2006). Over time, this increase in blood pressure causes mechanical stress to the vein wall and the valves, which could render valves incompetent and dilate the vessel lumen (vasodilation). Incompetent valves fail to prevent backflow of blood and—as a result—venous pressure increases further, causing greater mechanical stress and increasing reflux. Thus, a two-way causality between blood pressure and vasodilation occurs—that is, as one increases, so does the other. As a result, a loop is formed between the two phenomena as they exacerbate the effect of one another. Ultimately, this feedback loop between the venous pressure increase and dilation of the vein is thought to be the underlying cause of varicosities that eventually results in abnormal blood flow, deformed valves, and stretched vessel walls (Whiteley, 2011) (Figure 2). Recently, an evaluation of endothelial cell dysfunction and venous wall remodeling in chronic venous diseases has become a topic of discussion. According to a number of studies, evidence suggests that valve incompetence arises secondary to vessel dilation (Castro-Ferreira, Cardoso, Leite-Moreira, & Mansilha, 2018; Somers & Knaapen, 2006). Studies on the

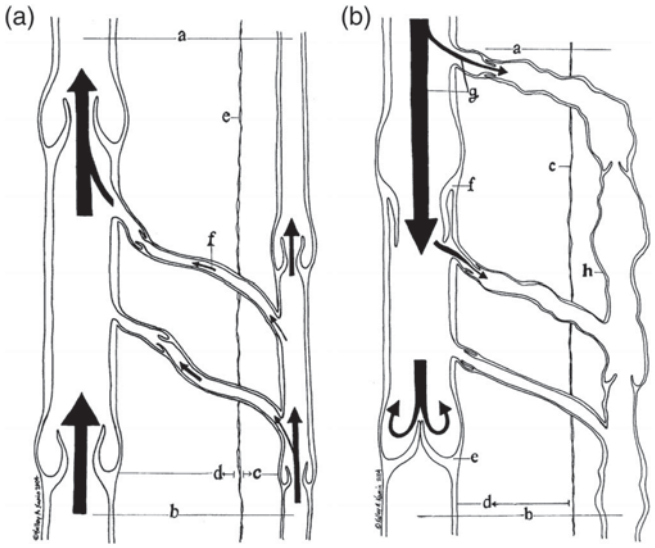

FIGURE 2 (A) Normal venous flow: (a) proximal, (b) distal, (c) superficial compartment, (d) deep compartment, (e) muscle fascia, (f) flow from superficial to deep veins. (B) Abnormal flow resulting from incompetent valves: (a) proximal, (b) distal, (c) muscle fascia, (d) deep compartment, (e) normal valve, (f) incompetent valve, (h) dilated superficial vein (Reprinted from Beebe-Dimmer, J. L. et al., Copyright [2005], with permission from Elsevier)

vessel wall of varicose veins—specifically on smooth muscle cells—highlighted compositional changes in vessel wall collagen, with an increase in collagen Type I and a decrease in collagen Type III. Collagens are important structural components responsible for vessel elasticity and compliance; notably, a decrease in collagen III would reduce the ability of veins to maintain their structural integrity and shape. Additionally, the increase in venous diameter due to venous reflux reduces wall shear stress, which in turn stimulates endothelial cells activating an inflammatory cascade. Despite these breakthroughs, it is likely that multiple interacting mechanisms are responsible for the development of varicose veins (Castro-Ferreira et al., 2018). Another study describes the histological differences of physiological and varicose veins in more detail (Oklu et al., 2012).

Varicose veins can occur anywhere in almost any part of the body, but the most susceptible vessels are superficial veins of the lower limbs, specially the great and small saphenous veins. This is due to their relatively larger diameter that allows them to contain greater volumes of blood, which may lead to a greater hydrostatic pressure (Zhang & Melander, 2014). A study showed that great saphenous veins that contain varicosities (n = 152) have a mean inner diameter of 6.39 ± 2.21 mm while normal great saphenous veins (n = 48) have a mean inner diameter of 4.41 ± 0.96 mm (Musil, Herman, & Mazuch, 2008). A number of studies have conducted rigorous investigations on the causality of varicose veins with respect to the hemodynamic insufficiencies of upstream veins (Recek, 2006, 2013, 2017). Varicose veins develop as a result of venous reflux, especially if it occurs in both deep and superficial veins. Contraction of muscles surrounding deep veins reduces deep vein reflux and the likelihood of developing deep vein varicosities; yet they do occur in extreme cases. Deep vein varicosities are mainly due to deep vein thrombosis—a condition that can arise in patients with advanced varicosities. Proper treatment and management of superficial varicose veins can minimize deep vein reflux (Lin, Zhang, Sun, Ren, & Liu, 2015). For a more detailed account, Whitely discusses current theories of venous reflux Whiteley, 2011.

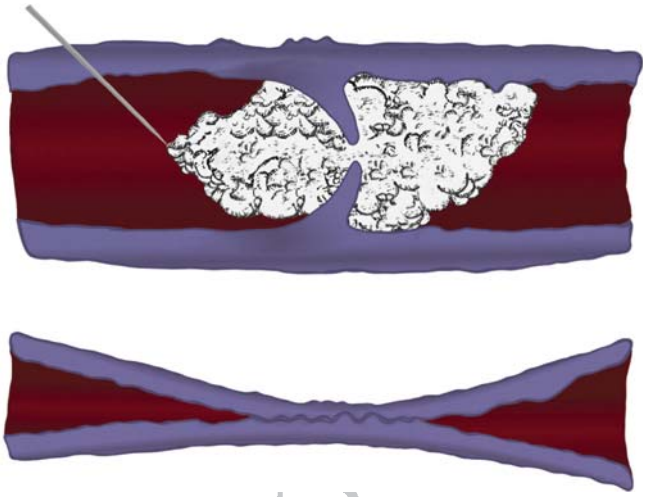

FIGURE 3 Foam sclerotherapy causes endothelial cell damage resulting in endovenous occlusion

Varicose veins affect more than 20% of the population in developed countries (Zhang & Melander, 2014). Although non-fatal, varicosities can affect a patient's quality of life significantly through symptoms such as leg swelling and fatigue, aching, muscle cramps, itchiness, and others (Zhang & Melander, 2014). The economic impact of venous ulcers corresponds to the 2% of the total healthcare budget of all Western countries (Cilurzo et al., 2019).Treatments are aimed at removal or destruction of the abnormal vein segments. They can be invasive (e.g., venous stripping), more painful (e.g., endovenous thermal ablation) or non-invasive (e.g., ultrasound-guided sclerotherapy). While reported adverse effects of sclerotherapy are fewer compared to other treatments, it can achieve similar outcomes with less pain and faster recovery (Carugo et al., 2013; Nastasa et al., 2015; Zhang & Melander, 2014).

3 | FOAM SCLEROTHERAPY

Sclerotherapy involves the injection of a surfactant solution—using a needle or a catheter—that damages the inner vessel wall. This process involves the activation of calcium signaling and nitric oxide pathways in response to the sclerosant's injection, causing endothelial cell lysis, vascular fibrosis, and subsequent endovascular occlusion (Figure 3) (Bottaro, Paterson, Zhang, et al., 2019; Carugo et al., 2013; Eckmann, 2009). Upon injection, the efficacy of liquid sclerosants decreases due to dilution and rapid deactivation by blood components, making liquid sclerotherapy ineffective when conducted on larger veins such as saphenous veins (Cameron, Chen, Connor, Behnia, & Parsi, 2013; Carugo et al., 2015). Studies have revealed that some of the injected sclerosant is consumed

by lysing of blood cells (erythrocytes, leukocytes and platelets in blood) (Connor, Cooley-Andrade, Goh, Ma, & Parsi, 2015), while blood proteins (e.g., serum albumin) can cause sclerosant deactivation (Watkins, 2011). An earlier study has experimentally demonstrated the binding of serum albumin to sclerosing agents such as sodium tetradecyl sulfate (STS) and polidocanol, leading to inhibition (Parsi et al., 2008). To overcome dilution and deactivation, the sclerosant is mixed with a gas and is administered in large veins as a foam (Bottaro, Paterson, Zhang, et al., 2019; Cameron et al., 2013; Carugo et al., 2015). The main benefit of administering sclerosing foams lies in their capacity to mimic a piston that displaces intravenous blood, leading to a greater contact surface area with venous endothelium, reduced mixing with blood and subsequent deactivation, and reduced staining of the leg due to trapped blood in the collapsed vessel (Carugo et al., 2015). A recent study attempted to create polidocanol-liposome nanoconstructs to further stabilize the resulting foam while minimizing interaction of the surfactant with plasma proteins (Cilurzo et al., 2019).

Foam sclerotherapy is also used to treat diseases such as oesophageal variceal, haemangioma, vascular malformation, hemorrhoids and cystic diseases (Zheng, Wei, & Zhang, 2018). Lately a new approach called ultrasound-guided foam sclerotherapy (UGFS) has gained popularity among clinicians. The benefits of UGFS include accurate placement of the needle within the venous lumen, demonstration of the path travelled by the foam plug, and the potential to observe spasm within treated vessels (Gibson & Gunderson, 2018). More recently, a novel technique known as sclerotherapy augmented phlebectomy (SAP) has been developed, which combines venous stripping of large varicose segments with sclerotherapy of smaller segments (Kolluri, Hays, & Gohel, 2018). Sclerotherapy is reported to be 32% cheaper than surgery (Belcaro et al., 2000). A study conducted in 2015 shows that sclerotherapy costs approximately £315 per session to the NHS (Marsden et al., 2015). According to the Vein Centre (United Kingdom), a private sclerotherapy treatment plan including consultation, foam sclerotherapy injection and compression stockings may cost up to a total of £800. If necessary, follow-up sessions would cost approximately £300 per session (Vein Centre, 2019). The following is an account on the production, formulation and clinical outcomes of sclerosing foam therapy.

3.1 | Methods of production

Various production methods may be utilized to produce sclerosing foams. Critello et al. (2019) includes a thorough review on such methods. This section summarizes these methods and various studies conducted to evaluate their performance.

3.1.1 | Conventional clinical methods

Physician compounded foams (PCFs) are generally produced using either the Double Syringe System (DSS) (Hamel-Desnos et al., 2003) or the Tessari method (Tessari, Cavezzi, & Frullini, 2001). Figure 4 shows the different connectors and syringe arrangements used for both methods. The general consensus is to use a smaller syringe for liquid surfactant and a larger syringe for gas (Tessari, 2002). Most commonly, a 5 ml syringe containing liquid surfactant and a 10 ml gas-filled syringe are used (Tessari et al., 2001). The surfactant solution is passed into and out of the 10 ml syringe 10 times, creating a foam (Carugo et al., 2015). It is suggested to use silicone-free syringes for foam production, as silicone reduces the half-life of foam by interfering with molecular links and the foam lamellae (half-life is defined as the time required for half of the liquid content of foam to drain) (Geroulakos, 2006). These techniques—although effective in producing a homogenous foam—lack the capability to make more than 10 ml of foam at a time, which may be a requirement for treatment of extensive lesions. Due to this bottleneck, a modified Tessari method (Figure 4c) has been proposed which is capable of delivering 20 ml of foam at a time (Xu, Wang, Chen, Wang, & Liu, 2016). Additionally, Bai et al. (2018, 2019) has created a laboratory-made automated machine to produce Tessari foam under constant pump speed and cycling rates in order to eliminate variability in foam properties (Figure 4d). There are no other studies that address the variability of PCF's properties due to inconsistent production criteria.

Depending on surfactant concentration (Bai et al., 2018), liquid-to-gas ratio—also referred to as foam quality in the literature (Cameron et al., 2013), method of production (Carugo et al., 2013; Critello et al., 2017), syringe type and needle size (Bottaro et al., 2019), and bubble size distribution—also referred to as size dispersity in the literature (Cameron et al., 2013; Carugo et al., 2016; Critello et al., 2017); the stability of the resulting foam can vary (Cavezzi & Tessari, 2009). An ideal sclerosing foam needs to be sufficiently cohesive, viscous, and with a low bubble size dispersity in order to exhibit stable characteristics (i.e., lower drainage time and slower rate of coarsening) (Star, Connor, & Parsi, 2018). It can be hypothesized that properties of PCFs could be user-dependent; in other words, the quality of the administered foam may highly depend upon the clinician's extent of experience and knowledge on ideal foam characteristics. With the aim of creating a foam with consistent characteristics, Provensis Ltd. (a BTG International group company—part of Boston Scientific) has developed a product known as Varithena® for the semi-automated preparation of a polidocanol injectable foam (previously referred to widely in the literature as polidocanol endovenous microfoam, or PEM, as we will use throughout this review for consistency with other publications) (Carugo et al., 2016).

3.1.2 | Polidocanol endovenous microfoam

Other than a study evaluating the effect of pumping speed on quality of the resulting Tessari foam (Bai et al., 2018), the scope of available research on alternative methods of sclerosing foam production is limited. PEM (commercially known as Varithena®) is the only semi-automated clinical production method developed for sclerotherapy purposes so far. The production method and formulation of PEM are

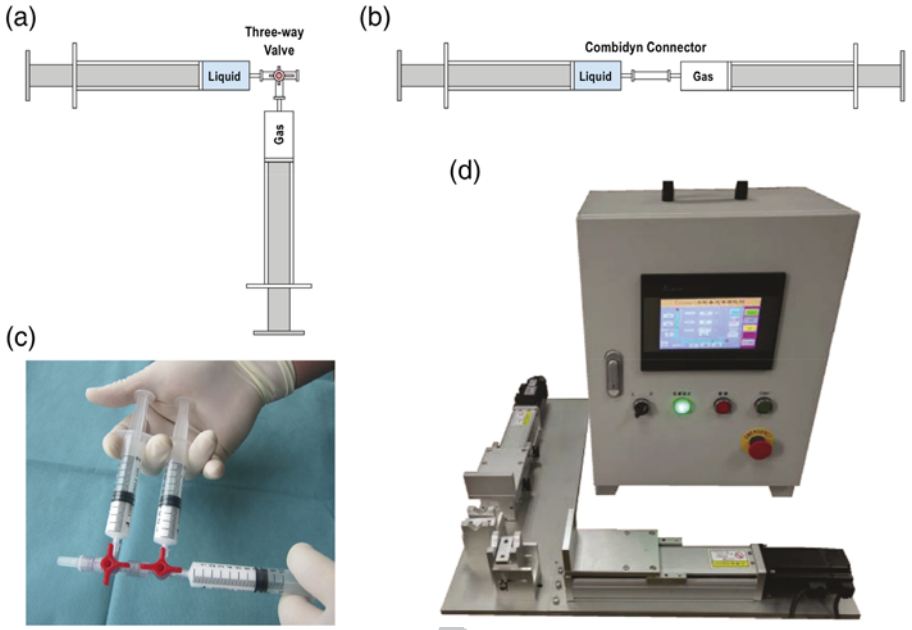

FIGURE 4 (a) The Tessari apparatus comprises of two syringes connected via a three-way stop-cock set at a 30° off-set. (b) The Double Syringe System (DSS) apparatus includes two syringes connected via a Combidyn connector (Figure adopted from [Carugo et al., 2016]), (c) The modified Tessari apparatus. One syringe is filled with liquid while the two parallel syringes are filled with gas. Three syringes are connected via two three-way stop-cocks (Reprinted from Xu et al., Copyright [2016], distributed under the terms of the Creative Commons Attribution 4.0 International License (http://creativecommons.org/licenses/by/4.0/)). (d) Laboratory-made automatic foam production device (Modified and Reprinted from Bai T. et al., Copyright [2019], with permission from Elsevier)

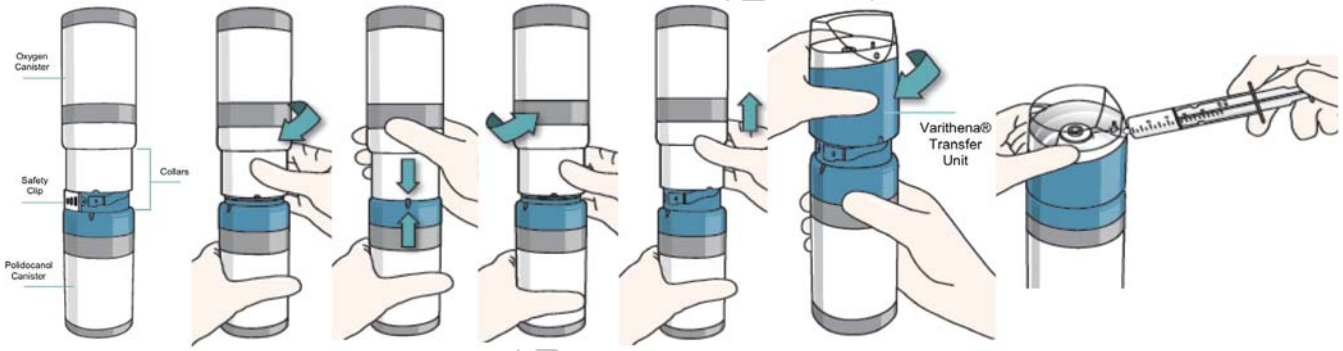

FIGURE 5 Varithena® canister contains all required components and is capable of readily producing PEM on demand. The gas canister is placed on top of the polidocanol cannister. By twisting the canisters together in a clockwise direction, gas is transferred to the polidocanol canister, creating PEM. The gas canister is then replaced with a Varithena® transfer unit which allows the withdrawal of foam into a syringe (Modified and Reprinted from Carugo D. et al., Copyright [2015], distributed under the terms of the Creative Commons Attribution 4.0 International License (http://creativecommons.org/licenses/by/4.0/))

rather different compared to PCFs. Most PCFs that are made using polidocanol surfactant use volumetric concentrations of 0.5–3% and room air at a 1:4 liquid to gas ratio (Carugo et al., 2016; de Oliveira, de Morais-Filho, Engelhorn, Kessler, & Neto, 2018; Rabe & Pannier, 2010; Yiannakopoulou, 2016) to create the desired foam, while PEM uses a 1% polidocanol solution (Carugo et al., 2015) at a 1:7 liquid to gas ratio to improve foam stability. Where PCFs benefit from stability of room air due to the low solubility of nitrogen, Varithena® produces PEM using a low nitrogen (<0.8%) gas combination of 35% CO_2 and 65% O_2 (Carugo et al., 2015; Star et al., 2018) in order to negate the issues of injection of nitrogen into the blood stream (Ceulen, Sommer, & Vernooy, 2008; Forlee, Grouden, Moore, & Shanik, 2006). A Varithena® canister assembly (Figure 5) automatically mixes gas and surfactant solution at the appropriate ratios, ensuring a consistent foam texture (bubble size distribution) and composition (Carugo et al., 2016). The formulation and production technique of sclerosing foams therefore is variable and impacts foam performance and ultimately clinical outcomes. Such studies are discussed in depth in Section 3.3.1. In addition to PEM, other separate studies report on the benefits of CO_2 containing sclerosing foams where a mixture of 30% O_2 and 70% O_2 is referred to as "physiological gas." It is reported that physiological gas can reduce the prevalence rates of skin irritation (Moneta, 2012) as well as significantly reducing the likelihood of other side-effects such as chest tightness and dry cough (Morrison et al., 2008; Wong, 2015) due to the greater solubility of CO_2 compared to N_2.

3.1.3 | Alternative methods of foam production

Although PCFs and PEM are currently utilized by clinicians, other foam production techniques exist which have never been used to produce sclerosing foams. It has been reported that foams can also be produced by mechanical agitation of a surfactant solution via acoustic cavitation, using either a tip sonicator (Critello et al., 2017) or under the effect of an ultrasound field in a non-flowing fluid system (Fiorillo, Fiorillo, Critello, & Pullano, 2015). A study demonstrated that low-frequency ultrasound can produce foams with smaller bubbles compared to PCF foams. Ninety-eight percentage of the bubbles were found to be smaller than 55 μm (mean of 19 μm) for the sonicated foam and 211 μm (mean of 37.1 μm) for the Tessari foam. The smaller bubble size may reduce the risk of neurological complications due to gas embolism post-treatment. Critello et al. extended their research to study the effect of sonication pulse parameters on foam stability. It was demonstrated that higher pulse duty cycles resulted in more stable foams, with the maximum stability observed for foams manufactured by continuous wave sonication mode at 10 s sonication time (foam half-life ≈ 100 s). Further sonication was found to continuously reduce foam half-life. Given that acoustic waves transfer energy to the surfactant solution, it would be logical for the internal energy of the solution to increase, resulting in an increase in temperature during the course of sonication that may, in turn, accelerate liquid drainage. As a result, a continuous wave sonication mode would reduce foam half-life over longer time periods (Critello et al., 2017).

Additional to sonication, conventional mechanical agitation of a surfactant solution can also be utilized for foam production. Critello et al. extended their study and characterized the stability and bubble size distribution of polidocanol foams produced via mechanical agitation of a 4% solution inside glass vials, at 4,300 rpm for 60 s. Foam half-life as a function of mixing time for foams with liquid to gas ratios of 1:1 and 1:2 showed that the 1:2 foam generated by conventional agitation had nearly double the half-life of the 1:1 foam. Comparison of foams generated via conventional agitation with those produced using a sonicator demonstrated the potential for sonication to produce foams with smaller bubbles that can be dissolved in blood more easily after administration, reducing the risk of gas embolization.

Depending on the agitation apparatus utilized, the production method may result in a different foam microstructure. For instance, mixing a surfactant solution with a spinning mixer at 5,000–10,000 rpm in a baffled container (Figure 6a) produces a closely packed bubble mixture of diameter ranging 10–100 μm, called a colloidal gas aphron (CGA) or a microfoam (Tseng, Pilon, & Warrier, 2006). CGAs have applications in the bioprocessing sector, namely fermentation in bioreactors, protein separation, and separation of metals or organic dyes from water (Larmignat, Vanderpool, Lai, & Pilon, 2008; Tseng et al., 2006). CGAs are different to other foam types in terms of bubble morphology. Where normal foam bubbles consist of a gas core coated by a monolayer of surfactant molecules, CGA bubbles were speculated to consist of a multilayer of surfactant and liquid (Figure 6b,c). This hypothesis was based on absence of the coalescence phenomena, and the fact that CGA bubbles produced in a dyed solution retain their color when transferred to a clear solution. This is now a proven hypothesis thanks to studies based on X-ray diffraction (Larmignat et al., 2008). CGAs are known to exhibit a low viscosity (similar to that of water) and can travel longer distances compared to conventional foams under identical experimental conditions. Furthermore, they do not exhibit extensive instabilities such as liquid drainage (Tseng et al., 2006). Nonetheless their application in sclerotherapy has not been explored yet.

3.2 | Clinical outcomes

The most common surfactants used in foam sclerotherapy (Figure 7) are STS and polidocanol (POL) (Cameron et al., 2013; de Oliveira et al., 2018; Rabe & Pannier, 2010), although other sclerosants used previously include glycerin, hypertonic saline and sodium morrhuate (Yiannakopoulou, 2016). Currently only STS, POL and sodium morrhuate are cleared by the FDA (Gibson & Gunderson, 2018).

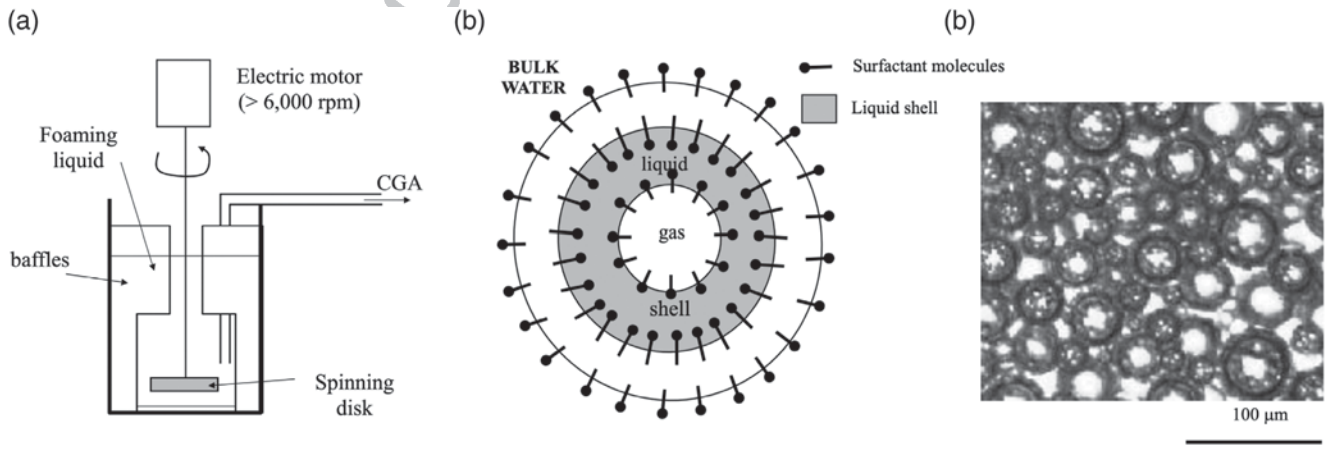

FIGURE 6 (a) Apparatus used for production of CGAs. (b) Schematic diagram of CGA bubble structure. (c) Micrograph of CGA bubbles (Reprinted from Tseng H. et al., Copyright [2006], with permission from Elsevier). CGA, colloidal gas aphron

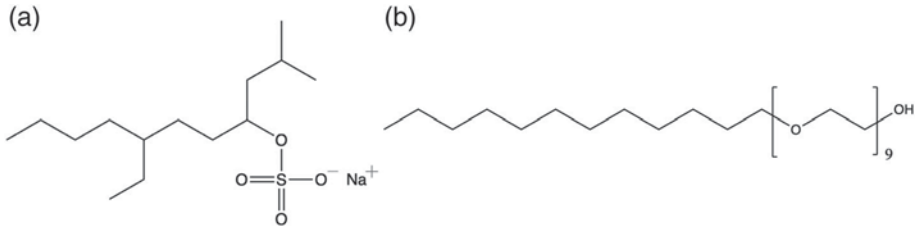

FIGURE 7 Skeletal structures of (a) STS and (b) POL

3.2.1 | Mechanism of action

In general, surfactants are compounds that contain a hydrophobic hydrocarbon chain and a hydrophilic head. They are classified into four groups: non-ionic, cationic (with a net positive charge), anionic (with a net negative charge), and zwitterionic (containing two oppositely charged head groups). POL is non-ionic whereas STS is anionic. The non-ionic nature of POL together with its long hydrocarbon chain make it a milder surfactant compared to STS which is known to be at least three times more potent than POL (Parsi, 2015). The clinical utility of surfactants relies on their ability to reduce the surface tension of a solution. For instance in foams, surfactant molecules adsorb at the gas-water interfaces, preventing coalescence of gas bubbles allowing for a more stable foam (Parsi, 2015). Injection of liquid or foamed sclerosant into vessels causes damage to vascular endothelium, transforming the pathological vessels into a fibrous cord and resulting in vessel sclerosis (Zheng et al., 2018). Considering the lipid bilayer structure of cell membranes, upon contact with the endothelium surfactant molecules interact with the membrane of endothelial cells and reduce its surface tension. As surfactant concentration increases within the vascular lumen, the lipid bilayer is eventually solubilized. According to Parsi, the surfactant-membrane interaction can be divided into four primary phases. At low surfactant concentrations, surfactant molecules diffuse into the membrane without disrupting it (Phase 1). As concentration increases, surfactant molecules aggregate within the lipid bilayer resulting in doughnut-shaped fragments (Phase 2). A further increase in surfactant concentration disrupts the cell membrane leading to solubilization and formation of smaller membrane sheets, as well as surfactant-lipid micelles (Phase 3). In the final phase, the cell membrane is completely fragmented and more micelles are formed (Phase 4). Membrane proteins may also be denatured depending on the surfactant used. For instance, ionic surfactants interfere with the surface charge of proteins which can lead to denaturation (Parsi, 2015).

3.2.2 | Foam therapeutic effects

Sclerotherapy transforms the varicose segment into a fibrous cord that in the case of small vessels fades over time, while in larger vessels—such as the great saphenous vein—the diameter is significantly reduced (Zheng et al., 2018). Whether valves regenerate following this treatment, at present remains unclear and no studies to date address this question. Furthermore, venous reflux is eliminated (de Oliveira et al., 2018). There is a gap in the literature on the extent of sclerosant diffusion into the vessel wall, and the fate of the treated vessel. Although sclerotherapy is relatively efficient in the short term, 70% of patients have been reported to exhibit varicosities up to 10 years post-treatment (Campbell et al., 2003). Evidently, sclerotherapy could potentially be optimized to result in more desirable outcomes. While invasive methods such as surgery and venous stripping can reduce recurrence rates by approximately 20% (Jones et al., 1996), the scope of research on optimization of non-invasive methods, such as sclerotherapy, is limited. According to a number of studies, varicose vein recurrence is due to neovascularization; that is, the formation of new blood vessels in response to ischemia via migration of endothelial cells to regions experiencing ischemia, resulting in a functional vascular network (Jones et al., 1996; Van Rij et al., 2004). Furthermore, histological analysis of varicose vein cells suggest that varicose endothelium exhibit abnormal morphologies (Somers & Knaapen, 2006). Thus, it can be hypothesized that any remaining abnormal endothelial cells post-sclerotherapy may migrate and proliferate to reform more varicose veins.

A number of reasons may be responsible for this treatment inefficiency; dilution of the injected foam or deactivation of sclerosant molecules during treatment could reduce lytic activity leaving some endothelial cells undamaged. In addition, it has been reported that buoyancy exerted by blood on the foam could reduce foam-vessel contact surface or cause inhomogeneous bubble size distribution (Cameron et al., 2013). In conclusion, it is crucial to maximize endothelial cell lysis during treatment. These challenges are addressed in Section 5.3 in more depth.

3.2.3 | Side effects

Sclerotherapy has been associated with a number of adverse events. Table 1 summarizes the side-effects of sclerotherapy (Yiannakopoulou, 2016; Zheng et al., 2018). The most common side effect has been reported to be pigmentation around treated blood vessels. A number of more serious effects can arise, namely deep vein thrombosis, neurological issues, and skin necrosis. Sclerotherapy has proven to result in lower incidence of embolic-related events compared to invasive procedures such as surgery (Zheng et al., 2018). Use of air has been reported to cause adverse neurological symptoms and increase the likelihood of gas embolism due to the low solubility of nitrogen in blood (Ceulen et al., 2008; Forlee et al., 2006). Additionally, visual disturbances have been reported to be more frequent after

TABLE 1 A list of the most common adverse events associated with sclerotherapy (liquid or foam) and their corresponding rate of incidence (Yiannakopoulou, 2016; Zheng et al., 2018)

Adverse event	Incidence rate
Dermal pigmentation	10–50%
Neovascularization	15–20%
Superficial thrombophlebitis	4–7.5%
Skin necrosis	0.23%
Arterial injury	18 cases
Stroke	16 cases
Visual disturbance	1.4–14%
Deep vein thrombosis	0.1–6%
Allergic reaction (non-fatal)	0.3%

foam sclerotherapy (Yiannakopoulou, 2016). It has also been reported that STS foam correlates with more pain and post-treatment skin ulcers, where POL can result in skin pigmentation (Ramadan, El-Hoshy, Shaaban, Hassan, & El-Sharkawy, 2011). Another study reports that both STS and POL can cause hyperpigmentation (Gibson & Gunderson, 2018).

The incidence of STS-related adverse events are greater than that of POL (Yiannakopoulou, 2016), which can be explained through the lower potency of POL relative to STS and may be the reason that POL is the only approved sclerosant in Europe (Zheng et al., 2018). Comparable studies carried out to determine the advantages of PEM over other PCFs are limited (Star et al., 2018), however, Phase 3 trials demonstrate that adverse neurological side-effects of PEM are clinically negligible (Todd et al., 2014).

3.3 | Chemical formulation

The focus of this section will be on POL-based foam due its aforementioned advantages.

3.3.1 | Effect of formulation on foam properties

Different production methods result in different bubble sizes in the manufactured foams. A recent study (Carugo et al., 2016) measured the bubble size distribution of different sclerosing foams, including PEM, 40 s after production. Results show the bubble diameters to be in the range 130–510 μm for DSS foams and 130–750 μm for Tessari foams generated using room air (1:7 liquid to gas ratio). Room air PCFs at 1:7 liquid to gas ratio generally exhibited a wider bubble size distribution compared to PEM; additionally, DSS foam showed a narrower bubble size distribution compared to Tessari. Furthermore the Tessari method was found to produce anomalously large bubbles (>1,000 μm in diameter). The narrower size distribution and the absence of abnormally large bubbles in DSS foams lead to the conclusion that they may be more cohesive, consistent, and stable compared to Tessari foams. Over time, foam microstructure ages and results in larger bubbles. Carugo et al. measured the effect of ageing on bubble size distribution and found that Tessari foams are more likely to result in larger bubbles compared to DSS foams. This study was extended to include PCFs with similar formulations to PEM (1:7 liquid to gas ratio, and a gas combination of 35:65 O_2:CO_2). The results show that PEM exhibits the narrowest size distribution (130–500 μm) compared to PCFs. After ageing, the PEM bubble size distribution shifts toward larger bubbles but it remains consistent with no bubbles >875 μm in diameter. The results of this study demonstrate that the gas composition is not the sole factor responsible for enhanced properties of PEM, but that the production mechanism for Varithena® (see Figure 7) also plays a crucial role in producing a consistent foam microstructure (Carugo et al., 2016). Other studies discuss the effect of needle size (Bottaro, Paterson, Quercia, et al., 2019), liquid-to-gas ratio (Cameron et al., 2013), and production techniques (Critello et al., 2017) on bubble-size distribution. Although these studies explore the microstructural and flow phenomena of sclerosing foams, as well as discussing microstructural differences between PEM and PCFs, there remains a gap in the literature on flow properties of sclerosing foams. Additionally, the relationship between surfactant concentration and bubble count and structure remains unexplored.

4 | PHYSICS OF AQUEOUS FOAM

Aqueous foams are multiphasic fluids comprising of gas bubbles dispersed in a solution of amphiphilic molecules called surfactants (Cohen-Addad, Höhler, & Pitois, 2013; Dollet & Raufaste, 2014; Gopal & Durian, 1999), which are adsorbed at the gas–liquid interface—also referred to as the liquid film (Cameron et al., 2013) (Figure 8a). Such foams have applications in ore extraction, oil recovery, food preparation, firefighting and cosmetics (Gopal & Durian, 1999; Herzhaft, 1999; Höhler & Cohen-Addad, 2005; Tseng et al., 2006). The ordered arrangement of surfactant molecules in the liquid films allows the foam structure to have a minimum interfacial energy density, though this can vary for foams of different liquid–gas ratios. Thus, the foremost parameter to define is the liquid volume fraction (ϕ_l)—the ratio of liquid volume to the total foam volume. At the close-packing fraction ($\phi_{l,c}$—liquid volume fraction of close-packing), gas bubbles are undeformed spheres and are almost touching one another. $\phi_{l,c}$ was determined numerically to be 0.0931 and 0.2595 for two-dimensional and three-dimensional emulsions (Princen, 1985). However, $\phi_{l,c}$ is not recognized as the threshold between wet and dry foams. As liquid volume fraction decreases below the close-packing fraction, gas bubbles deform and start to form polyhedral cells. At a low liquid volume fraction ($\phi_l \longrightarrow 0$) foam is said to be "dry" (see Figure 9b). In a dry foam, bubbles at equilibrium are bounded by a thin film of surfactant solution. These films satisfy Plateau's rules: films join in threes at a 120° angle forming the so-called Plateau borders that meet fourfold at nodes with 109.47° angles (Figure 8b) (Cohen-Addad et al., 2013). Surfactant molecules stabilize the foam structure by reducing surface tension of the liquid–

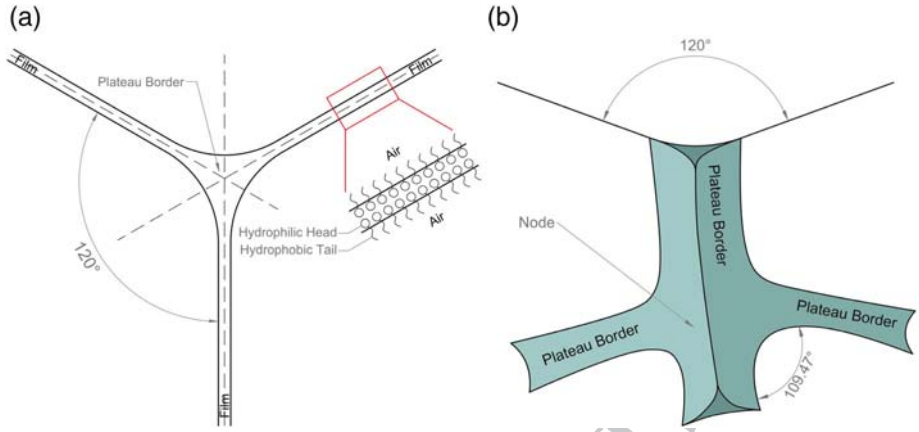

FIGURE 8 (a) Schematic of liquid films and Plateau borders. According to Plateau's rules, films meet threefold at an angle of 120° to form a Plateau border. Surfactant molecules provide stability to liquid films by arranging themselves at the gas–liquid interface. The hydrophilic heads point inwards toward the surfactant solution while the hydrophobic tails point toward the air. (b) Plateau borders meet at an angle of 109.47°, resulting in a tetrahedron configuration

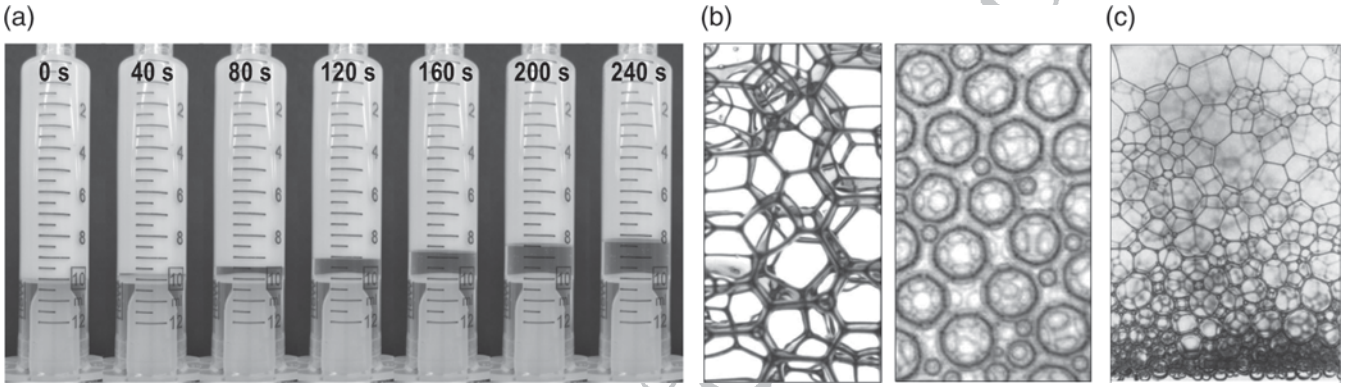

FIGURE 9 (a) An illustration of drainage (1% POL Tessari foam, 1:3 liquid to gas ratio). Over time the liquid fraction drains and pools at the bottom of the syringe. (b) Topological differences between dry (left) and wet (right) foams. In wet foams, the liquid films are thicker and bubbles are spherical whereas in dry foams, bubbles (cells) are polyhedral (Figure adopted from [Höhler & Cohen-Addad, 2005],© IOP Publishing. Reproduced with permission. All rights reserved, DOI: 10.1088/0953-8984/17/41/R01). (c) As foam drains, liquid pools at the bottom. As a result, the lower regions of foam are wetter compared to the higher regions (Used with permission of Royal Society of Chemistry, from Saint-Jalmes A., 2006; permission conveyed through Copyright Clearance Center, Inc.)

gas interface and repel bubbles away from each other (Saint-Jalmes, 2006).

4.1 | Ageing

Ageing refers to irreversible time-dependent changes occurring in the structure of stationary foams and is governed by various mechanisms. Ageing includes three synergistic phenomena: drainage, coarsening (also known as Ostwald Ripening) and coalescence (Saint-Jalmes, 2006).

4.1.1 | Drainage

In a dry foam ($\phi_l \longrightarrow 0$) all the liquid content of a foam is confined in the films, nodes and Plateau borders. Gravity causes the liquid to flow downwards resulting in thicker Plateau borders in lower regions. Consequently, the capillary pressure in the lower region increases according to the Laplace–Young law, inducing capillary flow upwards. Thus, the drainage of liquid out of the foam is governed by gravity and capillary forces (Figure 9). These two forces work against one another; however, gravity dominates capillary forces and liquid will inevitably flow downwards. A commonly used method in the literature to study drainage (known as "forced-drainage study") involves forcing the surfactant solution into drained dry foam at a given flow rate (Saint-Jalmes, 2006). More in-depth discussions of numerical models describing ageing and drainage of foams are given in (Karakashev, 2017; Parikh, 2017; Saint-Jalmes, 2006). CGAs are reported to age in a different manner compared to conventional aqueous foams. According to Tseng, where dry polyhedral foams exhibit capillary flow, dry CGAs lack such flows because bubbles retain their spherical morphology even in dry forms due to the presence of liquid within their multilamellar structure (Tseng et al., 2006).

4.1.2 | Coarsening

Gas diffusion through the liquid–gas interface (also referred to as Ostwald ripening in literature) is another mechanism that contributes to

F10 the evolution of aqueous foam structure (Figure 10a). The driving force behind diffusion is the difference in Laplace pressure of neighboring bubbles. Laplace pressure (i.e., the pressure difference between the inside and the outside of a bubble) is inversely proportional to bubble radius; as a result, gas diffuses from smaller bubbles (high pressure) into bigger bubbles (low pressure). This process is also referred to as a T2 event. A major consequence of coarsening is an increase in mean bubble diameter over time (Höhler & Cohen-Addad, 2005; Saint-Jalmes, 2006). It is reported that coarsening rate increases with gas solubility and gas volume fraction (Cohen-Addad et al., 2013). Figure 10b illustrates the effect of different gases on the rate of bubble coarsening. Nitrogen-based sclerosing foams are much more stable compared to oxygen based or carbon dioxide-based foams. Nitrogen contributes to foam stability due to its low solubility in water, although it may be responsible for adverse side-effects (Ceulen et al., 2008; Forlee et al., 2006). This has led to the notion that low nitrogen-content foams such as PEM could decrease the likelihood of adverse events, though statistical studies on clinical outcomes of PEM are yet to be carried out.

4.1.3 | Coalescence

After most of the liquid is drained, liquid films separating adjacent bubbles rupture, leading to bubble coalescence (Höhler & Cohen-Addad, 2005). It is important not to confuse coarsening with coalescence. Coalescence via film rupture is poorly understood and remains a prospective area of future studies (Saint-Jalmes, 2006); this may be the reason some studies refer to coarsening as coalescence (Parikh, 2017). During drainage, bubbles can simultaneously coarsen and coalesce (Höhler & Cohen-Addad,-2005; Saint-Jalmes, 2006). Karakashev et al. is one of only a few reports that has modeled liquid films and Plateau borders including the mechanism of coalescence (Karakashev, 2017).

4.1.4 | Synergy between ageing phenomena

Over time, the rate of all ageing processes decreases (Cohen-Addad et al., 2013). The physical and chemical attributes of foams such as surfactant formulation and liquid viscosity can be tuned to minimize drainage—the more viscous the liquid phase, the greater the viscous dissipation during drainage, hence the slower the rate of drainage (Saint-Jalmes, 2006; Saint-Jalmes & Langevin, 2002). A number of studies provide experimental data that correlate needle size (Bottaro, Paterson, Quercia, et al., 2019), foam type and production technique (Carugo et al., 2016; Critello et al., 2017), surfactant type (Bai et al., 2018) and concentration (Bai et al., 2018; Critello et al., 2017), and liquid-to-gas ratio (Cameron et al., 2013) with drainage time.

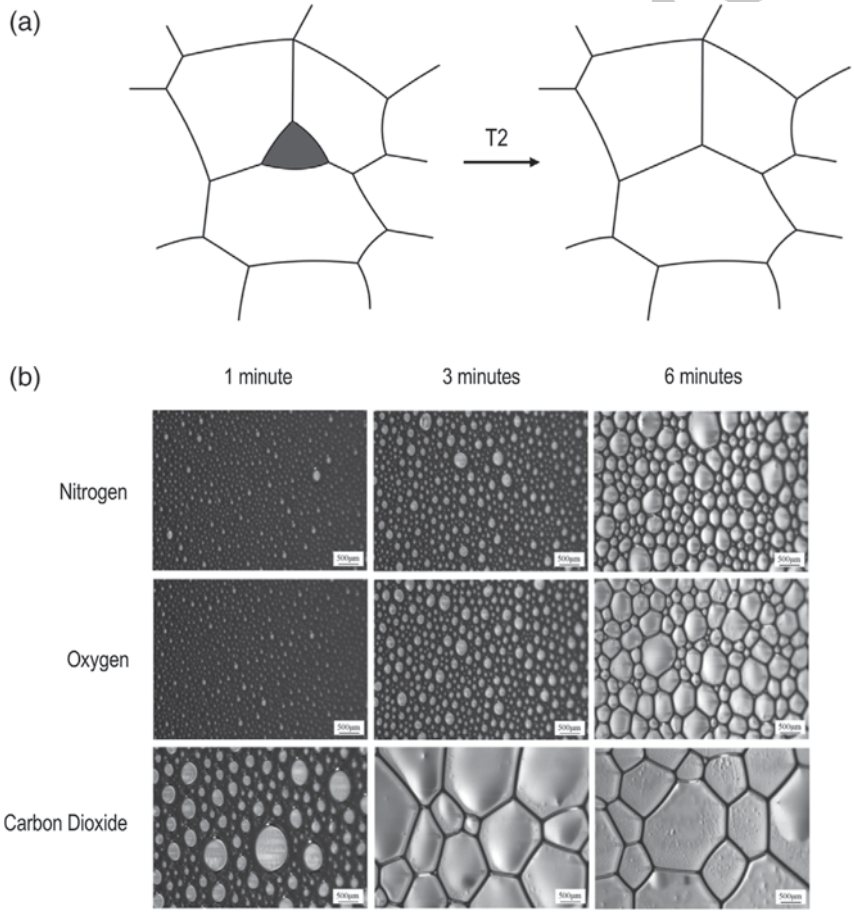

FIGURE 10 (a) T2 events (or Ostwald ripening) in 2D dry foams are also known as coarsening. (b) Sodium dodecyl sulfate [0.1% (wt/wt)] foam produced using different gases exhibits different rates of Ostwald ripening. Carbon dioxide is highly soluble in water; therefore, bubble size increases much more rapidly over time compared to bubbles in foams made using less soluble gases (Reprinted from Sun Y. et al., Copyright [2006] American Chemical Society, with permission from Langmuir)

The ageing phenomena described previously can intermingle and lead to synergistic effects. For instance, coarsening decreases bubble count, which in turn increases the liquid content in films resulting in greater downward flow of the liquid due to gravity (Saint-Jalmes, 2006). This coupling between drainage and coarsening would lead one to conclude that a more soluble gas would subsequently result in faster drainage. Coalescence would also reduce bubble count. Therefore, it would be reasonable to conclude that a lower surface tension would lead to rapid coalescence and in turn, faster drainage.

4.2 | Rheology

Rheological modeling of foam is not as simple as that of Newtonian fluids due to attributes such as yield stress, rheomalaxis, and wall slip. This section will provide a brief overview of these attributes while discussing possible simplifications that could be employed to characterize sclerosing foams more precisely. Aqueous foams are complex multiphasic fluids which exhibit solid-like and fluid-like behaviors simultaneously (Gopal & Durian, 1999). Mechanical and rheological studies prove the existence of viscoelastic as well as viscoplastic behaviors in liquid foams (Dollet & Raufaste, 2014; Kraynik, 1988).

4.2.1 | Microstructural evolution of shearing foam

Under an extremely small shear stress, foam structure resists flow. Instead, it deforms linearly with the applied stress in a reversible manner (viscoelasticity) (Gopal & Durian, 1999). As stress increases, flow occurs at the "yield stress" when bubble rearrangements take place resulting in plastic deformation (Figure 11a). The onset of deformation is defined by the so-called "T1 event" during which bubble rearrangements occur (Figure 11b). If the viscoelastic behavior of foams prior to yielding is to be neglected, foams can be thought of as viscoplastic materials with a yield stress (Kraynik, 1988).

4.2.2 | Rheological classification of aqueous foams

In a more concise manner, foams can be regarded as "elastoviscoplastic" materials (Cheddadi, Saramito, & Graner, 2012). An aqueous foam behaves as a pseudoplastic (shear-thinning) fluid with a yield stress (Cohen-Addad et al., 2013). Different methods have been developed for determination of yield stress, although the resultant values may differ, sometimes by more than one order of magnitude. This has lead researchers to believe that there is more than one type of yield stress (Dinkgreve, Paredes, Denn, & Bonn, 2016). The stress at which flow is initiated is called the "static yield stress" and is signified by the onset of bubble rearrangements. In contrast, "dynamic yield stress" is the smallest stress at which fluid stops flowing (Cohen-Addad et al., 2013; Dinkgreve et al., 2016).

The coupling between the ageing phenomena and shearing can give rise to time-dependent rheological effects due to the continuously evolving structure of foams, adding another layer of complexity to foam rheology. Consequently, rheological properties of foams depend on the deformation history as well as the shear rate. Literature refers to this time-dependent rheological behavior as "thixotropy." It is worth noting that the presence of static and dynamic yield stress is associated with thixotropic materials, whereas simple yield stress materials are known to exhibit no stress overshoot (as seen in Figure 11a) resulting in a well-defined yield stress (Dinkgreve et al., 2016). Figure 12 summarizes the classification of time-dependent rheologies. Originally, thixotropy referred to materials which microstructure progressively breaks down due to applied shear and slowly rebuilds at rest ("time-thinning"), although the term has been generally used to refer to all time-dependent rheologies (Barnes, 1997; Bekkour & Scrivener, 1998). Contrary to time-thinning behavior, some materials exhibit time-thickening or "anti-thixotropy" behavior (Hackley & Ferraris, 2001). Clay-based surfactants, yogurt and flocculant solutions are among materials with time-dependent rheology (Barnes, 1997). On the other hand, the foam structure evolves irreversibly; thus the term "rheomalaxis" is often used to describe

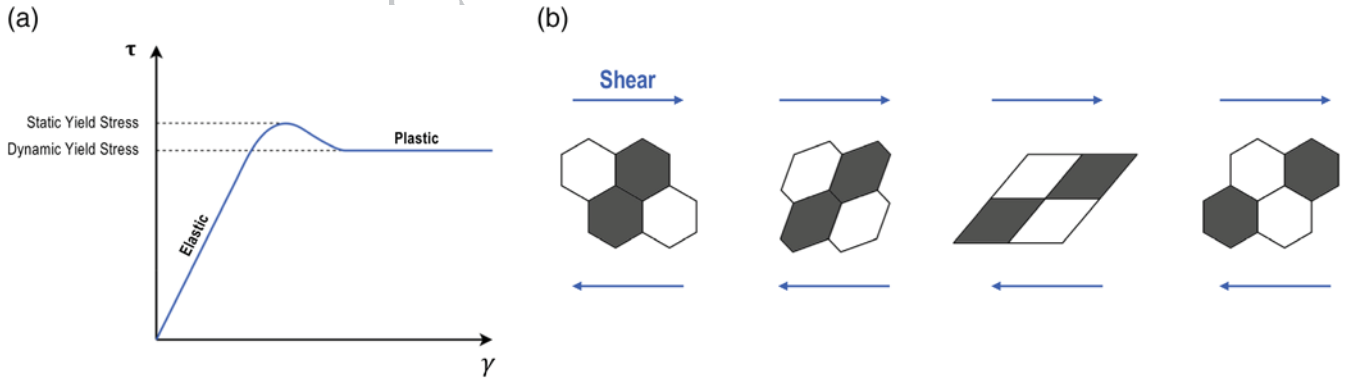

FIGURE 11 (a) Stress–strain curve of a foam demonstrates the initial elastic response as the linear segment. Flow is initiated when elasticity is replaced with plasticity. Static and dynamic yield stresses are illustrated (Adapted from [Cohen-Addad et al., 2013]). (b) T1 event is induced by a quasi-static increase in strain. During a T1 event, some films are shortened while others are lengthened, resulting in a mechanically unstable structure. Consequently, the bubbles rearrange while the structure relaxes into a more stable arrangement (Adopted from [Dollet & Raufaste, 2014])

such irreversible changes of viscosity over time (Bekkour & Scrivener, 1998; Hackley & Ferraris, 2001).

4.2.3 | Thixotropy

The most common method of measuring thixotropy is the hysteresis loop test. It involves a linear increase (loading) followed by a subsequent decrease (unloading) of shear rate (or shear stress) at constant shear stress (or shear rate) from zero to a predefined maximum value (Barnes, 1997; Hackley & Ferraris, 2001). Thixotropic and anti-thixotropic loops differ in relative positions of loading and unloading curves. As illustrated in Figure 13a, the loading curve of a thixotropic material lies above the unloading curve whereas for an anti-thixotropic material the unloading curve lies above the loading curve (Chhabra, 2010; Hackley & Ferraris, 2001). More in-depth discussion of time-dependent rheological models is provided in (Chhabra, 2010; de Souza Mendes, 2009; Hackley & Ferraris, 2001; Mujumdar, Beris, & Metzner, 2002).

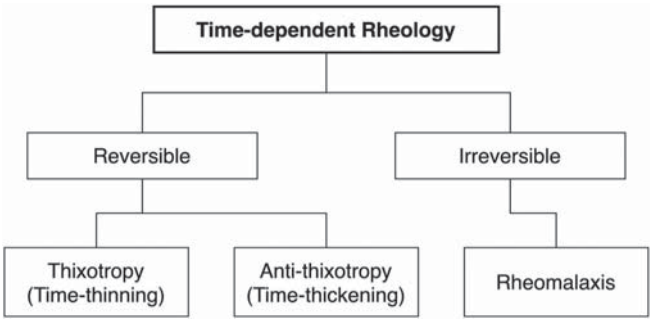

FIGURE 12 Classification of fluids with time-dependent rheological characteristics. Time-dependent rheology is either reversible or irreversible (also referred to as Rheomalaxis). Reversible rheological time-dependency can be Thixotropic where viscosity decreases with time (time-thinning) or anti-Thixotropic where viscosity increases with time (time-thickening). Aqueous foams are classified as Rheomalaxic material

A study investigated the time-dependent properties of sodium dodecyl sulphate (SDS) foam by carrying out a loop test. The results (Figure 13b) reveal the co-existence of both thixotropic and anti-thixotropic behaviors. The thixotropic (shear-thinning) behavior may be due to the onset of flow and a rearrangement of bubbles while coarsening events reduce the total number of bubbles, resulting in a reduction of interacting forces (Bekkour & Scrivener, 1998). Further increase in shear rate results in more frequent bubble break-up events, increasing interacting forces (Denkov, Tcholakova, Golemanov, Ananthpadmanabhan, & Lips, 2009). As a result, the bubble size distribution shifts toward smaller bubbles with an ever-increasing number of bubbles. This causes an increase in bubble interactions resulting in increasing viscosity with time (Bekkour & Scrivener, 1998). Denkov et al. provide intriguing discussions on the causality of bubble break-up (Denkov et al., 2009). Alternatively, time-dependent rheologies can be characterized by plotting loop surface area (thixotropic surface) as a function of stress ascent time (rate of change of shear stress). The results presented by Bekkour et al. (Figure 13c) show an increase in thixotropic surface with stress ascent time, suggesting that the bubble break-up events may be more pronounced with increasing stress ascent time (Bekkour & Scrivener, 1998).

Current literature includes other studies that attempt to model transient thixotropic effects; however these studies lack simplicity for product development purposes while their value as fundamental studies remains (de Souza Mendes, 2009; Mujumdar et al., 2002).

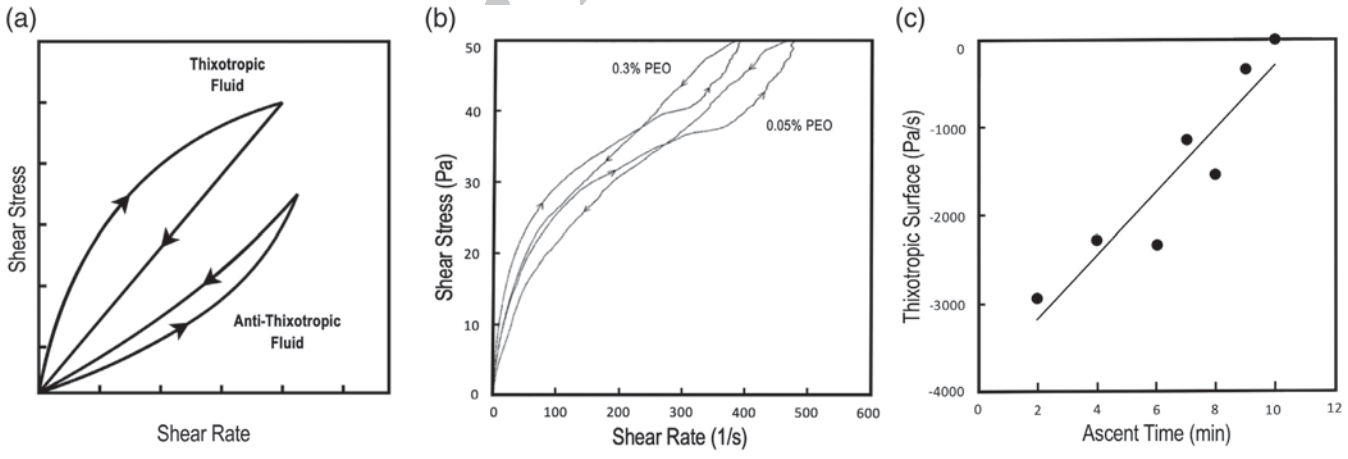

FIGURE 13 (a) Qualitative rheograms of thixotropic and anti-thixotropic fluids (Reprinted by permission from [Springer Nature]: [Springer] [Rheology of Complex Fluids] [Chhabra et al., Copyright (2010)]). (b) Hysteresis loop of 2% (wt/wt) SDS foam. Poly-ethylene oxide of different concentrations was used as stabilizer to minimize drainage (Reprinted by permission from [Springer Nature]: [Springer] [Mechanics of Time-Dependent Materials] [Bekkour et al., Copyright (1998)). (c) Thixotropic surface as a function of stress ascent time. The negative values of thixotropic surface mean that the area under the unloading curve is greater than the area under the loading curve. With increasing ascent time, bubble break-up is more pronounced given the little time bubbles have to equilibrate capillary and viscous forces (Reprinted by permission from [Springer Nature]: [Springer] [Mechanics of Time-Dependent Materials] [Bekkour et al., Copyright (1998)])

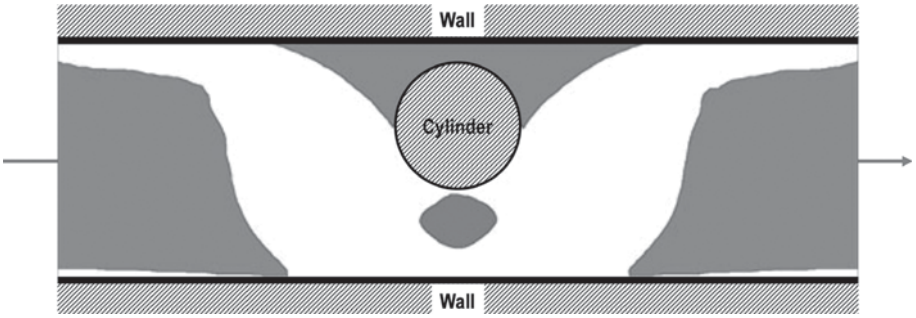

FIGURE 14 Numerical simulation results corresponding to creeping flow of a Bingham fluid in a partially occluded channel under a no-slip boundary condition. The occlusion (cylinder) is placed with a slight offset from the centerline, with fluid flowing from left to right. It is clear that obstructions in flow pathway of yield-stress fluids can result in unyielded (shaded) regions as opposing to flowing (white) regions (Reprinted from Denn M. et al., Copyright [2010], distributed under the terms of the Creative Commons Attribution Noncommercial License (https://creativecommons.org/licenses/by-nc/2.0))

Additionally, current models fail to distinguish thixotropy from viscoelasticity (de Souza Mendes, 2009). Among the reviewed models, Mendes proposes a simple and inclusive set of equations that include structure break-up, structure evolution under steady-state flow as well as a viscosity function that includes both static and dynamic yield stresses (de Souza Mendes, 2009).

4.2.4 | Complications of rheomalaxis

Rheomalaxic flow in tubular structures will inevitably result in complications such as the wall slip phenomena. When a fluid undergoes laminar flow in a tube (i.e., Poiseuille flow), shear rate increases with the distance from the tube centerline. In other words, the foam near the wall experiences the greatest shear rate. This results in rapid structure breakdown, causing the formation of a liquid film between the bulk foam and the tube that is responsible for the wall slip phenomenon (Barnes, 1997). It has been reported that foams under Poiseuille flow can exhibit a plug-flow behavior as a consequence of the wall slip phenomenon during which the bulk material does not experience deformation (Bertola, Bertrand, Tabuteau, Bonn, & Coussot, 2003; Herzhaft, 1999). A number of numerical and experimental methods exist that tackle the wall slip problem that will be discussed later in Section 5.1.6.

4.2.5 | Shear banding

In addition to time-dependent rheologies, events such as localization have been observed in foam rheometry. Localization or shear banding refers to the coexistence of stationary (solid) regions and flowing (liquid) regions (Cheddadi et al., 2012; Coussot et al., 2002; Debrégeas, Tabuteau, & Di Meglio, 2001) that occur when there is a shear stress gradient during flow. As a result, fluid regions experiencing a stress less than the yield stress remain stationary while the rest of the fluid flows (Denn & Bonn, 2011). Denn et al. have numerically demonstrated the existence of shear banding during flow of a Bingham fluid in a partially occluded channel at Re = 0 (Denn & Bonn, 2011) (Figure 14). Even though a zero Reynold's number is unrealistic, shear banding may still occur as a result of occlusions. Considering that venous valves may cause a partial reduction of the vein lumen, it may be reasonable to assume that shear banding occurs in these regions during foam sclerotherapy. Moreover, the role of yield stress in the efficacy of sclerotherapy has not been explored, although it can be anticipated that in sclerosing foams with a greater yield stress, shear banding would be more pronounced with a higher volume of stagnant foam in proximity of occlusions inside the vein lumen. Whether or not this would improve or compromise treatment outcome remains an unanswered question. Many studies demonstrate various techniques for yield stress calculation (Khan, Schnepper, & Armstrong, 1988; Kraynik, 1988; Princen & Kiss, 1989; Rouyer, Cohen-Addad, Vignes-Adler, & Höhler, 2003; TA Instruments, 2000). Dinkgreve et al. summarizes the most accurate of these techniques (Dinkgreve et al., 2016).

5 | PHYSICAL CHARACTERIZATION OF SCLEROSING FOAMS

The most fundamental studies of foam and emulsion rheology are the works of Khan et al. (Khan et al., 1988; Khan & Armstrong, 1986, 1987) and Princen et al. (Princen, 1983, 1985; Princen & Kiss, 1986, 1989). Khan et al. (Khan et al., 1988; Khan & Armstrong, 1986, 1987) developed a theory of stress tensor for deformation of monodisperse (i.e., constant bubble size) 2D dry foams, assuming a hexagonal foam cell geometry. This was then extended to polydisperse (i.e., variable bubble size) foams and further studies on yield stress. Results showed that yield stress increases with gas volume fraction (Khan et al., 1988) and is independent of cell size distribution about a constant mean (Khan & Armstrong, 1987). Princen's approach was to develop an elastic stress–strain relationship as a function of gas volume fraction and bubble contact angle for 2D foams (Princen, 1983, 1985) that was extended to 3D foams (Princen & Kiss, 1986, 1989). This resulted in a numerical expression for yield stress as a function of interfacial tension (i.e., surfactant solution), gas volume fraction and an empirical contribution of each bubble to bulk stress (Princen, 1983). The resulting model

was empirically validated in the presence of wall slip (Princen, 1985). The final results included an expression for effective viscosity of 3D foam as a function of bubble size, interfacial tension, viscosity of continuous phase and yield stress (Princen & Kiss, 1989). More recently, Denkov et al. (Denkov et al., 2009; Denkov, Subramanian, Gurovich, & Lips, 2005; Denkov, Tcholakova, Golemanov, Ananthapadmanabhan, & Lips, 2008; Denkov, Tcholakova, Golemanov, Subramanian, & Lips, 2006) extended the work done by Princen et al. (Princen, 1983, 1985; Princen & Kiss, 1986, 1989) by developing a foam-wall friction model evaluating the effects of wall surface mobility (i.e., smooth wall surface vs. roughened surface) (Denkov et al., 2005), gas volume fraction (Denkov et al., 2006), surfactant type and bubble surface mobility (Denkov et al., 2009). The work of Denkov et al. (Denkov et al., 2005, 2006, 2008, 2009) includes an in-depth physical model of aqueous foams proposed in the literature; however, the level of complexity of its equations makes it difficult to be widely applied for development of new sclerosing products. An overview of current clinically applicable modeling techniques is discussed below along with their corresponding limitations and advantages with respect to sclerosing foam development.

5.1 | Current theoretical and experimental methods

The aforementioned studies are the cornerstones of foam physics, yet the scope of their application in the evaluation of sclerotherapy is limited. We therefore describe in detail methods for measuring the rheological properties of foams that may be critical to their performance as sclerosing agents and we point the reader to the work of Chhabra (2010) which provides additional thorough review of the general rheology of non-Newtonian fluids.

5.1.1 | Conventional rheometry

In conventional rheometers, the fluid of interest undergoes Couette flow between two parallel plates (see Figure 15a for a representation of the velocity profile in Couette flow). Rheometers are of two types: controlled shear rate or controlled shear stress, depending on user choice of the appropriate independent variable. The most frequently used equation for modeling yield stress materials is the Herschel–Bulkley (HB) model (Cheddadi et al., 2012; Cohen-Addad et al., 2013):

$$\tau = \tau_y + K\dot{\gamma}^n \quad (1)$$

where τ is shear stress (Pa), $\dot{\gamma}$ is shear rate (s^{-1}), τ_y is yield stress (Pa), K is fluid consistency index, and n is fluid flow index. An exponent of 1 would reduce the HB model to the linear Bingham model for yield stress fluids (Dollet & Raufaste, 2014), whereas $n > 1$ and $n < 1$ correspond to pseudoplastic (shear-thinning) and dilatant (shear-thickening) behaviours (Björn, de La Monja, Karlsson, Ejlertsson, & Svensson, 2012). Note that in the absence of yield stress ($\tau_y = 0$), Equation (1) would reduce to the power-law equation ($\tau = K\dot{\gamma}^n$) (Chhabra, 2010).

A simple mathematical manipulation of Equation (1) would yield:

$$\ln(\tau - \tau_y) = n.\ln(\dot{\gamma}) + \ln(K) \quad (2)$$

Fitting stress data obtained from a controlled shear rheometer on a plot of $\ln(\tau - \tau_y)$ versus $\ln(\dot{\gamma})$ would be sufficient to calculate the consistency and flow indices of a given foam. Given that yield stress is the y-intercept of a $\tau - \dot{\gamma}$ graph, it may be determined by extrapolation of shear stress as shear rate approaches zero on a $\ln(\tau - \tau_y) - \ln(\dot{\gamma})$ plot (Marze, Langevin, & Saint-Jalmes, 2008). Studies report that most aqueous foams exhibit pseudoplasticity given that they report a flow index in the range $0.2 \lesssim n \lesssim 0.5$ (Cohen-Addad et al., 2013; Denkov et al., 2005; Dollet & Raufaste, 2014; Höhler & Cohen-Addad, 2005; Marze et al., 2008), although the range of values for n are said to be dependent on the rigidity of the gas–liquid interface (Cohen-Addad et al., 2013). Dollet et al. provides a more in-depth discussion on the interpretation of flow index values (Dollet & Raufaste, 2014). It is worth noting that the flow and consistency indices of sclerosing foams have never been calculated and remain unknown.

5.1.2 | Oscillation rheometry

An alternative to conventional rheometry is the application of oscillatory shear. As opposed to a linear increase in shear rate, this

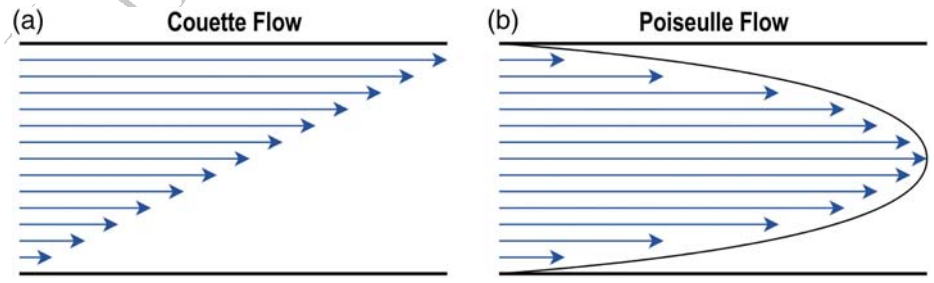

FIGURE 15 (a) Couette flow of a fluid between two parallel plates exhibits a linear velocity profile. The fluid travels between moving plates that applies shear stress while the other plate remains stationary. This concept is utilized in conventional rheometers. (b) Poiseuille flow of a fluid inside a tube exhibits a parabolic velocity profile with maximum velocity at the tube centerline and minimum velocity at tube walls. Poiseuille flow is the closest simplification of vascular flow and is the most biomimetically applicable flow model

technique involves subjecting the foam to a sinusoidal shear given by $\gamma = \gamma_0 \sin(\omega t)$ where ω and γ_0 are angular frequency and strain amplitude (Bair et al., 2014; Dollet & Raufaste, 2014). The oscillatory stress response is therefore given by:

$$\tau = \gamma_0 [G' \cos(\omega t) + G'' \sin(\omega t)] \quad (3)$$

where G' and G'' are storage and loss moduli that quantify elastic deformation and viscous dissipation respectively. Stress–strain curves obtained using this method show a clear transition from a viscoelastic response below yield stress to a non-linear power-law response, thus making this method desirable for yield stress determination (Dinkgreve et al., 2016). This method could be applied to measure the yield stress of sclerosing foams using rheometers which has never been done before. As it will be discussed later, rheometry of aqueous foam is error-prone due to the wall slip phenomena which can be eliminated by pasting sandpaper on the rheometer walls.

5.1.3 | Classification of rheological models

With a few exceptions (see below), almost all studies of foam rheology use rheometers as the primary experimental apparatus. These studies divide into three major categories, the third of which is of particular interest to sclerosing foam development.

First are studies with the aim of macroscopic modeling of foam's flow behavior. This includes conventional rheometric studies that employ the HB or the power-law model (Bertola et al., 2003; Kroezen, Wassink, & Schipper, 1988; Marze et al., 2008) while others apply the oscillatory shear method (Doraiswamy et al., 2002; Katgert, Tighe, & Van Hecke, 2013; Marze et al., 2008). Some studies have coupled magnetic resonance imaging (MRI) (Coussot et al., 2002), nuclear magnetic resonance (NMR) (Raynaud et al., 2002) or diffusive-wave spectroscopy (Gopal & Durian, 1999; Marze et al., 2008) with conventional rheometers to gain an understanding of the structural evolution of shearing foams.

The second group aims to study the microstructural events in a foam through the development of numerical theories of rheology that involve stress contribution per foam cell, viscous dissipation, inertial and capillary forces, and so forth (Denkov et al., 2005, 2008, 2009; Khan et al., 1988; Khan & Armstrong, 1986, 1987; Princen, 1983, 1985; Princen & Kiss, 1986, 1989). These studies also use rheometers to validate their models. Almost all of the reviewed articles here use rotational rheometers that are equipment of different geometries such as the cone-plate, Couette and concentric cylinders (Song, Salehiyan, Li, Lee, & Hyun, 2017). Although the results of rheometric studies are of great value from a physical characterization perspective, they are irrelevant to clinical procedures. In other words, rotational rheometers lack the capability of mimicking the bio-physical environment of sclerotherapy. This coupled with the challenge of thixotropic characterization, raises concerns regarding the validity of such equipment to study sclerosing foams. In other words, flow of foam in veins leads to a different deformation history than in rheometers. A more biomimetic setting is therefore required to characterize foams in more clinically relevant settings, leading us to the final category.

5.1.4 | Poiseuille rheometry

The third category of studies employs "Poiseuille rheometry" (also referred to as pipe viscometry) (Bekkour & Scrivener, 1998; Enzendorfer et al., 2002; Gardiner, Dlugogorski, & Jameson, 1998; Larmignat et al., 2008; Tseng et al., 2006). This has received attention specifically from the petroleum industry due to its potential to mimic industrial conditions (Herzhaft, 1999). The same potential makes Poiseuille rheometry an attractive route of experimental study for foam sclerotherapy. In contrast to conventional rheometers that utilize Couette flow, Poiseuille rheometry utilizes Poiseuille flow which is more relevant to vascular flow (Figure 15b), and also allows quantification of wall slip. Current protocols on pipe rheometry of CGAs (Larmignat et al., 2008; Tseng et al., 2006) and foams used in firefighting (Gardiner et al., 1998) and petroleum industry (Herzhaft, 1999; Herzhaft, Kakadjian, & Moan, 2005) are well-developed.

Poiseuille rheometry requires pipe lengths of various diameter fitted with at least two pressure sensors (one fitted at the inlet and one at the outlet). Volumetric flow rate (Q in m^3/s) is defined as the independent variable while the pressure drop across the pipe (ΔP in Pa) is recorded as the dependent variable. For Newtonian fluids under laminar flow in a pipe of diameter d and length L, the Hagen–Poiseuille equation relates pressure drop to viscosity (μ):

$$\mu = \frac{\Delta P \pi d^4}{128 Q L} \quad (4)$$

Although Equation (4) can provide estimates of foam viscosity, it does not account for the non-Newtonian behavior of foam or the wall slip phenomena. The volumetric flow rate and pressure drop may however be used to calculate apparent wall shear rate ($\dot{\gamma}_{observed}$) and wall shear stress (τ_w) (Gardiner et al., 1998):

$$\dot{\gamma}_{observed} = \frac{32Q}{\pi d^3} \quad (5)$$

$$\tau_w = \frac{d\Delta P}{4L} \quad (6)$$

Plotting τ_w against $\dot{\gamma}_{observed}$ would yield a rheogram, the gradient of which would be equal to the foam's apparent viscosity at any particular shear rate. However, Poiseuille flow assumes a no-slip boundary condition at the walls; as discussed in Section 4.2.4, wall slip is present during Poiseuille flow and needs to be quantified.

5.1.5 | Wall slip correction

An inevitable complication of foam flow in a pipe is the wall slip phenomenon. Given the shear-thinning nature of blood (Nanda et al., 2017), wall slip is not only a likely phenomenon in physiological

vessels, but also it has been attributed to vascular malformations such as microaneurysms (Drapaca, 2018). A consequence of wall slip is inconsistent shear rate calculations for a constant pressure drop over different pipe diameters (Herzhaft, 1999). Khan et al. (1988) eliminated wall slip by pasting sandpaper on the rheometer walls, although sandpaper would be impossible to paste inside a pipe. In order to eliminate slippage effects in pipes, numerical methods have been developed capable of computing wall slip velocity. For foam Poiseuille rheometry, the Oldroyd–Jastrzebski correction method has given consistently reasonable results. It assumes that wall slip velocity (u_{slip}) is directly proportional to wall shear stress and inversely proportional to pipe diameter (Equation 7) (Enzendorfer et al., 2002; Larmignat et al., 2008).

$$u_{slip} = \frac{\tau_w \beta(\tau_w)}{d} \tag{7}$$

where $\beta(\tau_w)$ is the slip coefficient, which itself is a function of τ_w. Equation (7) is then subtracted from the apparent shear rate in order to compute the true shear rate. True shear rate is calculated from Equation (8):

$$u_{observed} = u_{true} + u_{slip} \tag{8}$$

Note that while cross sectional area $A = \frac{\pi d^2}{4}$ and linear velocity $= \frac{Q}{A}$, Equation (5) by can be manipulated to yield:

$$\dot{\gamma} = \frac{32Q}{\pi d^3} = \frac{8Q}{d} \times \frac{4}{\pi d^2} = \frac{8Q}{dA} = \frac{8u}{d} \tag{9}$$

Keeping Equation (9) in mind while multiplying Equation (8) by $8/d$, and substituting Equation (7) into Equation (8) yields:

$$\dot{\gamma}_{observed} = \dot{\gamma}_{true} + \frac{8\tau_w \beta(\tau_w)}{d^2} \tag{10}$$

Equation (10) implies that a plot of $\dot{\gamma}_{observed}$ against $1/d^2$ must yield a straight line. The slip coefficient is then computed by dividing the slope ($8\tau_w\beta(\tau_w)$) by $8\tau_w$ and is subsequently plotted against wall shear stress. Curve fitting models are then used to find the relationship between slip coefficient and wall shear stress (least square fit, if directly proportional) to find the equation of the line $\beta(\tau_w) = a\tau_w + b$. Finally, the corrected true shear rate is calculated by rearranging Equation (10):

$$\dot{\gamma}_{true} = \dot{\gamma}_{observed} - \frac{8\tau_w(a\tau_w + b)}{d^2} \tag{11}$$

The Oldroyd–Jastrzebski slip correction has proven efficient at collapsing $\tau_w - \dot{\gamma}_{true}$ curves into a master curve independent of pipe diameter (Bekkour & Scrivener, 1998; Enzendorfer et al., 2002; Gardiner et al., 1998; Larmignat et al., 2008).

5.1.6 | Volume equalization

Finally, there is one last technique which can normalize the data corresponding to foams of different liquid to gas ratios; namely the "volume equalization" method. It was originally reported that the power-law equation can be normalized with respect to the specific expansion ratio (ε, defined as the ratio of liquid density to foam density) (Valkó & Economides, 2002):

$$\frac{\tau_w}{\varepsilon} = K_{VE}\left(\frac{\dot{\gamma}_{true}}{\varepsilon}\right)^n \tag{12}$$

Equation (12) has been shown to be capable of collapsing the *SD* of curves corresponding to foam of various gas volume fractions and ultimately allow the determination of a volume-equalized fluid consistency index (K_{VE}) and flow index. Previous studies demonstrate that foam viscosity increases with gas fraction (i.e., drier foams are more viscous) (Osei-Bonsu, Shokri, & Grassia, 2016). The most thorough experimental procedures of Poiseuille rheometry are included in (Enzendorfer et al., 2002; Larmignat et al., 2008). Volume equalization can be applied to foams produced using different methods in order to obtain method-specific flow and consistency indices.

Wall slip is a phenomenon that certainly occurs during the injection of sclerosing foams in varicose veins. Given the lack of rheological data on sclerosing foams in the literature, it is important to conduct wall slip correction during the rheological characterization of sclerosing foams in order to obtain the most accurate results. Volume equalization can then be applied to wall slip corrected data in order to compare viscosity values corresponding to foams of different liquid-to-gas ratios.

5.2 | In silico models

Recent advances in computational modeling have spawned a generation of in silico models that attempt to study various aspects of structural evolution in foams. A number of studies employ Surface Evolver (open source); a numerical modeling software that allows determination of random dry foam topology associated with the minimum interfacial energy density (Cox, 2005; Evans, Kraynik, Reinelt, Mecke, & Schröder-Turk, 2013; Kraynik, Reinelt, & van Swol, 2003, 2004). Surface Evolver is capable of simulating cell-level events, but it does not allow rheological modeling in tubes or vessels. Another technique is molecular dynamics (MD), which aims to simulate events at a molecular level and has been used to calculate interface formation energies and surface concentration per surfactant molecule in liquid films (Jang & Goddard, 2006). Another study used MD to evaluate the effect of different foaming gases (N_2, O_2, and CO_2) on interfacial phenomena such as gas diffusion and coalescence in SDS foams. Transient simulation in MD showed that CO_2 molecules interact with both the hydrophobic and hydrophilic ends of surfactant molecules, which allows them to permeate through the liquid films more rapidly. As a

result, channel openings in foam films were observed, which could accelerate CO_2 diffusion even further (Figure 16). Simulation results were then verified experimentally where CO_2 foams showed the highest rate of coalescence (refer to Figure 10) (Sun, Qi, Sun, Zhao, & Li, 2016). MD simulations can also potentially shed more light on the mechanism of interaction between surfactants and cell membranes.

In contrast to MD, a numerical software such as ANSYS® could prove insightful for modeling rheology and multiphasic flow of foams in a continuous phase. To this end, Wong et al. has employed a computational fluid dynamics (CFD) model to simulate sclerosing foam injection into a varicose vein. Foam was simulated as a "pseudo-fluid" via the volume of fluid (VOF) model in ANSYS® Fluent (Wong, Chen, Connor, Behnia, & Parsi, 2014), while bulk rheological properties of foam were selected based on previous experimental findings (Wong et al., 2015). The in silico results were then compared with experimental findings to evaluate the accuracy of the model in capturing foam's behavior. It was demonstrated that CFD could capture foam behavior to a reasonable degree of accuracy when injected into a straight channel; however, CFD's accuracy of simulating injection into a branched system was limited (Wong et al., 2014).

Although software packages such as Surface Evolver or MD show potential in capturing microstructural phenomena with a reasonable degree of accuracy, CFD modeling of foam remains underdeveloped. This could be due to lack of experimental data on fundamental rheological parameters and models of aqueous foams. Moreover, a CFD package often offers time-dependent viscosity models, which may be able to capture foam behavior more accurately, although experimental characterization is due prior to computational time-dependent

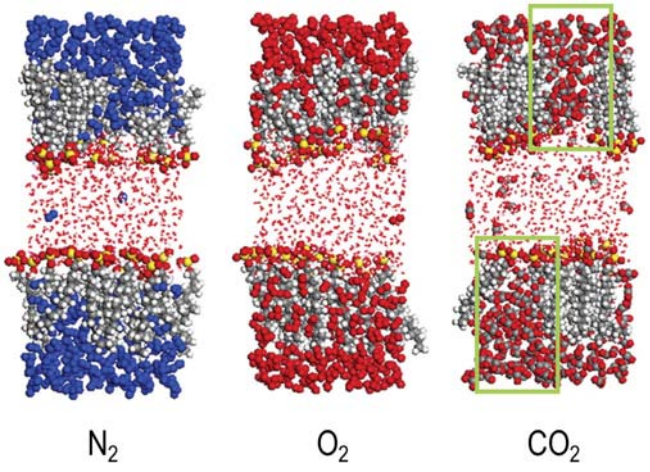

FIGURE 16 Molecular dynamics simulation results of a water phase flanked by two surfactant (SDS) monolayers with hydrophilic ends of surfactant placed inside the water phase. Two gas monolayers were positioned near the hydrophobic groups of SDS. As illustrated above, CO_2 molecules diffuse at a higher rate compared to N_2 and O_2 molecules. Furthermore, CO_2 molecules are shown to aggregate inside the surfactant monolayer, creating a "channel" opening (green rectangles) that could ultimately contribute to faster coarsening rates (Adapted and reprinted from Sun Y. et al., Copyright [2006] American Chemical Society, with permission from Langmuir)

models. Older in silico models of foams, such as the Potts and the "bubble" model, are briefly described in Höhler et al., which are not within the scope of this review (Höhler & Cohen-Addad, 2005).

There is also a growing demand to eliminate animal testing that can be replaced with in silico models; however, the capability of current models to simulate foam flow is yet to be fully studied. Recently, organizations such as the Food and Drug Administration (FDA) have formulated new guidelines that accept CFD methods in the research and development pipeline of new medical treatments (Bluestein, 2017). Various studies have attempted CFD modeling of blood flow in vessels. A number of studies carried out fluid–structure interaction simulations of vascular blood flow across two-dimensional (Amindari, Saltik, Kirkkopru, Yacoub, & Yalcin, 2017; De Hart, Peters, Schreurs, & Baaijens, 2000) and three-dimensional (De Hart, Peters, Schreurs, & Baaijens, 2003) aortic valves, and three-dimensional venous valves (Buxton & Clarke, 2006). The primary aims of these studies were to model the phenomena occurring during each cycle of valve function. Nevertheless, simulation studies of physiological vessel geometries could recreate the mechanics of blood flow—referred to as "hemodynamics." Such in silico studies could be used to gain a better insight on the propagation of foam after injection into varicose veins. This would require a more accurate rheological characterization of foams, as well as physiological varicose vein geometries. 3D venous geometries in the literature are almost all created empirically as opposed to physiologically. Recently, more specialized vascular CFD software, such as SimVascular© (SimVascular Development Team), have been developed to carry out vascular reconstruction from CT scans (Updegrove et al., 2017). Although other software packages such as Simpleware© (Synopsys®) have been previously used to reconstruct vascular geometries, SimVascular is specialized for vascular reconstruction as it is specifically designed to segment vessels and create centerlines to construct a continuous architecture. SimVascular also includes a CFD solver (Updegrove et al., 2017).

5.3 | Optimizing sclerotherapy

Based on the reviewed literature thus far, the scope of foam characterization studies with respect to end-point applications (sclerotherapy or otherwise) is limited compared to fundamental physical studies. Only a handful of studies have focused on characterizing foam physics in application-relevant setups that are discussed here. On a general note, reported studies have investigated the effect of foam production technique (Bottaro, Paterson, Zhang, et al., 2019; Carugo et al., 2015; Critello et al., 2017), syringe size and number of pumping cycles (Bai et al., 2018; Nastasa et al., 2015), surfactant concentration (Cameron et al., 2013; Wong et al., 2015) and temperature (Bai et al., 2018), different liquid to gas ratios (Cameron et al., 2013; Carugo et al., 2015; Wong et al., 2015) and various gas types (Carugo et al., 2013, 2015; Hashimoto, Uchida, Horikawa, Mimura, & Farsad, 2018) on characteristics of sclerosing foams such as bubble count, bubble size distribution and static half-life. The issue taken with these approaches is the relevance of attributes such as drainage time

and bubble properties to clinical performance of sclerotherapy. Although these parameters can characterize a foam physically, they do not directly reflect the lytic activity of sclerosing foams. Thus, optimization of sclerotherapy demands more clinically relevant parameters.

Carugo et al. (2013, 2015, 2016) developed a biomimetic quantitative characterization method coupled with an in-house computational foam analysis system ("CFAS") developed using MATLAB (The MathWorks, Inc.). A finite volume of POL PCFs of different compositions were injected at different rates into a PTFE tube primed with a blood substitute solution (30% v/v glycerol in water) while capturing real-time videos of foam propagation through the tube. During injection, the foam front propagates through the tube and subsequently degrades after complete injection. Recorded videos were analyzed and segmented by the CFAS. Outputs include a foam plug expansion rate (represented by the gradient of the expansion phase), and a foam degradation rate (gradient of the degradation phase) (Figure 17). The intriguing aspect of this work is the introduction of a new parameter that could directly reflect sclerosing foam performance—the so called "dwell time," which is defined as the inverse of the degradation rate. Dwell time (s/mm) represents the time in seconds that every unit length of tube wall is in contact with foam. Carugo et al. employed this technique to compare PEM with different PCFs (of similar gas composition to PEM) and found that PEM results in approximately a twofold and threefold increase in dwell time compared to DSS and Tessari foams (Carugo et al., 2015). PEM also exhibited a longer half-life and a narrower bubble size distribution (Carugo et al., 2016). The experimental method developed in these studies along with the dwell time parameter are the most clinically relevant approaches for characterizing sclerosing foams.

An alternative approach to the use of biomimetic straight tubes is to conduct experiments on polydimethylsiloxane (PDMS) based physical vein models (PVM) seeded with human umbilical vein endothelial cells (HUVECs) to create a biologically active environment. The PVM geometry includes a 3D venous geometry with a circular cross-section. Bottaro et al. used PVM devices mimicking physiological and varicose veins coupled with a modified version of the CFAS developed by Carugo et al. to determine the performance of PCFs. Furthermore, Bottaro et al. showed that DSS foams demonstrate greater dwell times in the varicose PVM, while both Bottaro et al. and Carugo et al. demonstrate that DSS foams are more stable and exhibit longer dwell times in general. In conclusion, dwell time analysis reveals that foam performance from best to worst is PEM > DSS > Tessari (Bottaro, Paterson, Zhang, et al., 2019).

Another important attribute of sclerosing foams is viscosity. Being a measure of resistance to flow, viscosity can directly reflect sclerosing foam performance once correlated with biological outcomes of sclerotherapy. Wong et al. employed cone-plate viscometry of POL Tessari foams, at shear rates of 0.01 s^{-1}–1 s^{-1}. Results included an estimated value of foam viscosity (~60 Pa.s corresponding to 1% POL foam with a 1:4 liquid-to-gas ratio); however, the study did not provide a clear indication of the stress–strain fitting method employed. Comparisons between foams of different liquid-to-gas

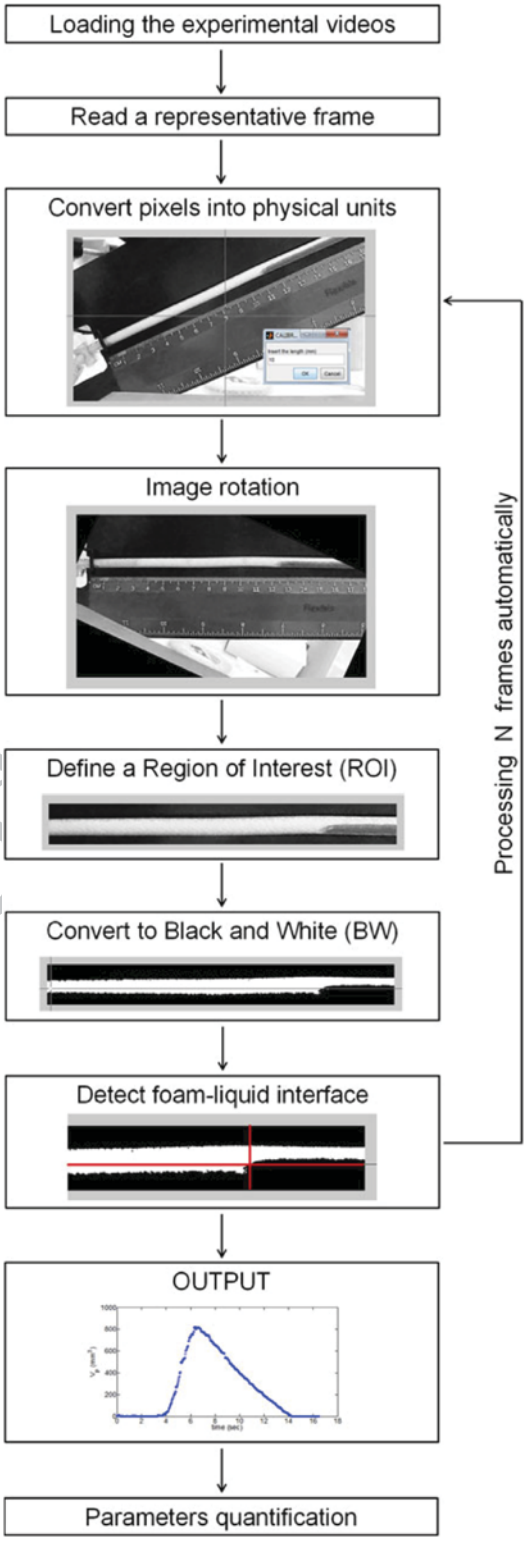

FIGURE 17 Sequence of operations carried out in the CFAS developed by Carugo et al. starts with reading the recorded video of foam propagation inside a transparent tube. A representative frame is selected, and pixels are converted to length units. The frame is then rotated, a region of interest is defined, and the image is binarised to contain only black and white pixels. Subsequently, the foam's front is detected, and its propagation is plotted against time (Reprinted by permission from [Springer Nature]: [Springer] Journal of Materials Science: Materials in Medicine] [Carugo et al., Copyright (2013)])

ratios confirmed an increase in foam viscosity with increasing gas fraction (Wong et al., 2015). Other research on foam viscosity in literature study the effect of stabilizing agents such as tween, xanthan gum, glycerine (Nastasa et al., 2015) and sulodexide (Critello, Fiorillo, Cristiano, de Franciscis, & Serra, 2019).

In contrast to these rheometric experiments, pipe viscometry experiments are being conducted in our labs by injecting sclerosing foams into a polytetrafuoroethylene (PTFE) tube of defined length. Preliminary results have revealed that sclerosing foams identical to that used by Wong et al. exhibit Poiseuille viscosities ranging from 0.05 Pa.s (corresponding to shear rate of 700 s^{-1}) to 0.27 Pa.s (corresponding to shear rate of 80 s^{-1}). This is in accordance with the previously observed shear-thinning behavior of aqueous foams. Physiological wall shear rate in veins ranges from about 20 s^{-1} to 200 s^{-1} (Hathcock, 2006; Shi et al., 2016). Given the pseudoplasticity of aqueous foams and the reduced shear rate in varicose veins due to venous reflux, viscosity values corresponding to shear rates lower than 20 s^{-1} are thus likely to be less relevant to venous flow inside varicose veins; nevertheless, lack of clinical data on operational attributes of sclerotherapy—such as injection flow rate and the extent of vein compression during treatment—make it difficult to anticipate the range of observed shear rates experienced by sclerosing foams during treatment.

6 | FINAL REMARKS

Recurrence of varicosities due to migration of endothelial cells that survive sclerotherapy suggests that there is room for improvement in the lytic activity of sclerosing foams. Additionally, reported side-effects may be addressed through treatment optimization. Due to the increasing number of physical studies on foam structure during the past four decades, our understanding of foam microstructural phenomena has reached a developed stage. Attributes such as yield stress give rise to shear banding while transient microstructural events result in a time-dependent rheology. Although studies of these events have proven to be of great fundamental value, more clinically relevant parameters such as dwell time are needed to measure performance of sclerosing foams. While physical characterization of foams still remains imperfect, it is possible to optimize the performance of sclerosing foams in biomimetic settings such as PVMs. Future research directions could address the following challenges:

- Pipe viscometry of sclerosing foams remains an unstudied topic. Apparent viscosity is a parameter that could be used as an independent variable in future studies against other clinically relevant variables such as dwell time or lytic activity within physiologically relevant shear rates. Furthermore, replicating surface properties of vessels in in vitro studies is crucial in order to accurately replicate the interaction between foam and vessel wall.
- There may be other clinically relevant properties of foams that need to be studied. Other than dwell time, the capability of a known volume of foam to displace blood could be a potentially useful parameter. This may be correlated with rheological properties of sclerosing foams such as viscosity. Moreover, PCFs (all foams other than Varithena®) are formulated in-house prior to administration, and user-variability is a factor that can also affect lytic activity.
- Surfactant drainage after injection could potentially affect treatment outcomes. It is unclear how fast liquid is drained from shearing foam during sclerotherapy. Further studies are needed in order to characterize the extent of foam dilution and mixing with blood after injection.
- The complexity of current thixotropic models prohibits transient viscous phenomena from being considered relevant to clinical outcomes. Hysteresis loop tests have not been carried out on sclerosing foams. The loop surface area may prove to be an important parameter to study and correlate with lytic activity. For the time being, simple experimental modifications such as pre-shearing, may prove effective at minimizing thixotropic effects. Pre-shearing involves the shearing of foam under controlled conditions for a short period of time to allow the foam to reach dynamic equilibrium before conducting primary experiments. This also allows the formation of the liquid film around the foam plug responsible for wall slip.
- The possibility still exists that parameters such as flow index, yield stress, loss and storage moduli of sclerosing foams are relatable to clinical outcomes. These parameters are yet to be quantified accurately.
- PVMs could benefit from clinical imaging data in order to create more accurate varicose vein models. Future in silico studies may utilise specialist software in order to create accurate vascular geometries.
- While molecular dynamics simulations have proven to accurately explain microstructural events such as coarsening, they can also be utilized to study the surfactant-cell interaction. Such studies are yet to be undertaken.
- CFD simulations are yet to be improved upon in order to capture macrostructural flow of foams. However, they can be used to extract an approximate propagation path of the foam plug after injection. To this end, a more accurate viscous characterization of foam is required as well as biomimetic varicose vein geometries.

ACKNOWLEDGMENTS

Authors would like to thank the Engineering and Physical Sciences Research Council (EPSRC), for having contributed to fund Alireza Meghdadi's PhD studentship through an EPSRC DTP scheme (awarded by the Faculty of Engineering and the Environment, University of Southampton). We also thank Mr. Masih Motamedvaziri for creating the illustration of foam sclerotherapy (Figure 3).

CONFLICT OF INTEREST

Stephen A. Jones, Venisha A. Patel, and Andrew L. Lewis are employees at Biocompatibles Ltd. (a BTG International group company), and they are working on the development of Varithena.

GLOSSARY

Shear stress (τ)	force per unit area perpendicular to the cross section of the fluid conduit which deforms the fluid without changing its volume
Shear rate ($\dot{\gamma}$)	the rate at which fluid layers slide past one another
Rheogram	a plot of shear stress versus shear rate whose gradient represents apparent viscosity at that specific shear rate
Reynolds number (Re)	a dimensionless figure that characterizes the flow regime of a given fluid flowing at a given flow rate in a given pipe

ORCID

Alireza Meghdadi https://orcid.org/0000-0001-6805-7183
Andrew L. Lewis https://orcid.org/0000-0001-5779-5631

REFERENCES

Amindari, A., Saltik, L., Kirkkopru, K., Yacoub, M., & Yalcin, H. C. (2017). Assessment of calcified aortic valve leaflet deformations and blood flow dynamics using fluid-structure interaction modeling. *Informatics in Medicine Unlocked*, *9*, 191–199. https://doi.org/10.1016/j.imu.2017.09.001

Bai, T., Jiang, W., Chen, Y., Yan, F., Xu, Z., & Fan, Y. (2018). Effect of multiple factors on foam stability in foam sclerotherapy. *Scientific Reports*, *8*(1), 15683. https://doi.org/10.1038/s41598-018-33992-w

Bai, T., Liu, Y., Liu, J., Yu, C., Jiang, W., & Fan, Y. (2019). A comparison of different surfactants on foam stability in foam sclerotherapy in vitro. *Journal of Vascular Surgery*, *69*(2), 581–591.e1. https://doi.org/10.1016/j.jvs.2018.02.033

Bair, S., Yamaguchi, T., Brouwer, L., Schwarze, H., Vergne, P., & Poll, G. (2014). Oscillatory and steady shear viscosity: The Cox-Merz rule, superposition, and application to EHL friction. *Tribology International*, *79*, 126–131. https://doi.org/10.1016/j.triboint.2014.06.001

Barnes, H. A. (1997). Thixotropy—A review. *Journal of Non-Newtonian Fluid Mechanics*, *70*, 1–33. https://doi.org/10.1016/S0377-0257(97)00004-9

Beebe-Dimmer, J. L., Pfeifer, J. R., Engle, J. S., & Schottenfeld, D. (2005). The epidemiology of chronic venous insufficiency and varicose veins. *Annals of Epidemiology*, *15*(3), 175–184. https://doi.org/10.1016/j.annepidem.2004.05.015

Bekkour, K., & Scrivener, O. (1998). Time-dependent and flow properties of foams. *Mechanics Time-Dependent Materials*, *2*(2), 171–193. https://doi.org/10.1023/A:1009841625668

Belcaro, G., Nicolaides, A. N., Ricci, A., Dugall, M., Errichi, B. M., Vasdekis, S., & Christopoulos, D. (2000). Endovascular sclerotherapy, surgery, and surgery plus sclerotherapy in superficial venous incompetence: A randomized, 10-year follow-up trial—Final results. *Angiology*, *51*(7), 529–534. https://doi.org/10.1177/000331970005100701

Bertola, V., Bertrand, F., Tabuteau, H., Bonn, D., & Coussot, P. (2003). Wall slip and yielding in pasty materials. *Journal of Rheology*, *47*(5), 1211–1226. https://doi.org/10.1122/1.1595098

Björn, A., de La Monja, P. S., Karlsson, A., Ejlertsson, J., & Svensson, B. H. (2012). Rheological characterization. *Biogas*, *InTech*. https://doi.org/10.5772/32596

Bluestein, D. (2017). Utilizing computational fluid dynamics in cardiovascular engineering and medicine-what you need to know. Its translation to the clinic/bedside. *Artificial Organs*, *41*(2), 117–121. https://doi.org/10.1111/aor.12914

Bottaro, E., Paterson, J. A. J., Quercia, L., Zhang, X., Hill, M., Patel, V. A., … Carugo, D. (2019). In vitro and ex vivo evaluation of the biological performance of sclerosing foams. *Scientific Reports*, *9*(1), 9880. https://doi.org/10.1038/s41598-019-46262-0

Bottaro, E., Paterson, J., Zhang, X., Hill, M., Patel, V. A., Jones, S. A., … Carugo, D. (2019). Physical vein models to quantify the flow performance of sclerosing foams. *Frontiers in Bioengineering and Biotechnology*, *7*. https://doi.org/10.3389/fbioe.2019.00109

Buxton, G. A., & Clarke, N. (2006). Computational phlebology: The simulation of a vein valve. *Journal of Biological Physics*, *32*(6), 507–521. https://doi.org/10.1007/s10867-007-9033-4

Cameron, E., Chen, T., Connor, D. E., Behnia, M., & Parsi, K. (2013). Sclerosant foam structure and stability is strongly influenced by liquid air fraction. *European Journal of Vascular and Endovascular Surgery*, *46*(4), 488–494. https://doi.org/10.1016/j.ejvs.2013.07.013

Campbell, W. B., Vijay Kumar, A., Collin, T. W., Allington, K. L., Michaels, J. A., & Randomised and Economic Analysis of Conservative and Therapeutic Interventions for Varicose veins Study. (2003). The outcome of varicose vein surgery at 10 years: Clinical findings, symptoms and patient satisfaction. *Annals of the Royal College of Surgeons of England*, *85*(1), 52–57. https://doi.org/10.1308/003588403321001462

Carugo, D., Ankrett, D. N., O'Byrne, V., Willis, S., Wright, D. D. I., Lewis, A. L., … Zhang, X. (2013). A novel biomimetic analysis system for quantitative characterisation of sclerosing foams used for the treatment of varicose veins. *Journal of Materials Science: Materials in Medicine*, *24*(6), 1417–1423. https://doi.org/10.1007/s10856-013-4913-6

Carugo, D., Ankrett, D. N., O'Byrne, V., Wright, D. D. I., Lewis, A. L., Hill, M., & Zhang, X. (2015). The role of clinically-relevant parameters on the cohesiveness of sclerosing foams in a biomimetic vein model. *Journal of Materials Science: Materials in Medicine*, *26*(11), 258. https://doi.org/10.1007/s10856-015-5587-z

Carugo, D., Ankrett, D. N., Zhao, X., Zhang, X., Hill, M., O'Byrne, V., … Lewis, A. L. (2016). Benefits of polidocanol endovenous microfoam (Varithena®) compared with physician-compounded foams. *Phlebology*, *31*(4), 283–295. https://doi.org/10.1177/0268355515589063

Castro-Ferreira, R., Cardoso, R., Leite-Moreira, A., & Mansilha, A. (2018). The role of endothelial dysfunction and inflammation in chronic venous disease. *Annals of Vascular Surgery*, *46*, 380–393. https://doi.org/10.1016/j.avsg.2017.06.131

Cavezzi, A., & Tessari, L. (2009). Foam sclerotherapy techniques: Different gases and methods of preparation, catheter versus direct injection. *Phlebology*, *24*(6), 247–251. https://doi.org/10.1258/phleb.2009.009061

Recek, C. (2017). Insights into the venous hemodynamics of the lower extremity. *Clinics in Surgery*, *2*, 1452.

Ceulen, R. P. M., Sommer, A., & Vernooy, K. (2008). Microembolism during foam sclerotherapy of varicose veins. *New England Journal of Medicine*, *358*, 1525–1526. https://doi.org/10.1056/NEJMc0707265

Cheddadi, I., Saramito, P., & Graner, F. (2012). Steady Couette flows of elastoviscoplastic fluids are nonunique. *Journal of Rheology*, *56*(1), 213–239. https://doi.org/10.1122/1.3675605

Chhabra, R. P. (2010). Non-Newtonian fluids: An introduction. In *Rheology of complex fluids* (pp. 3–34). https://doi.org/10.1007/978-1-4419-6494-6_1

Cilurzo, F., Critello, C. D., Paolino, D., Fiorillo, A. S., Fresta, M., de Franciscis, S., & Celia, C. (2019). Polydocanol foam stabilized by

liposomes: Supramolecular nanoconstructs for sclerotherapy. *Colloids and Surfaces B: Biointerfaces*, *175*, 469–476. https://doi.org/10.1016/j.colsurfb.2018.12.027

Cohen-Addad, S., Höhler, R., & Pitois, O. (2013). Flow in foams and flowing foams. *Annual Review of Fluid Mechanics*, *45*(1), 241–267. https://doi.org/10.1146/annurev-fluid-011212-140634

Connor, D. E., Cooley-Andrade, O., Goh, W. X., Ma, D. D. F., & Parsi, K. (2015). Detergent sclerosants are deactivated and consumed by circulating blood cells. *European Journal of Vascular and Endovascular Surgery*, *49*(4), 426–431. https://doi.org/10.1016/j.ejvs.2014.12.029

Coussot, P., Raynaud, J. S., Bertrand, F., Moucheront, P., Guilbaud, J. P., Huynh, H. T., … Lesueur, D. (2002). Coexistence of liquid and solid phases in flowing soft-glassy materials. *Physical Review Letters*, *88*(21), 2183011–2183014. https://doi.org/10.1103/PhysRevLett.88.218301

Cox, S. J. (2005). A viscous froth model for dry foams in the surface evolver. *Colloids and Surfaces A: Physicochemical and Engineering Aspects*, *263*, 81–89. https://doi.org/10.1016/j.colsurfa.2004.12.061

Critello, C. D., Fiorillo, A. S., Cristiano, M. C., de Franciscis, S., & Serra, R. (2019). Effects of sulodexide on stability of sclerosing foams. *Phlebology*, *34*(3), 191–200. https://doi.org/10.1177/0268355518779844

Critello, C. D., Pullano, S. A., Matula, T. J., de Franciscis, S., Serra, R., & Fiorillo, A. S. (2019). Recent developments on foaming mechanical and electronic techniques for the management of varicose veins. *Expert Review of Medical Devices*, *16*, 931–940. https://doi.org/10.1080/17434440.2019.1682549

Critello, C. D., Fiorillo, A. S., & Matula, T. J. (2017). Size of sclerosing foams prepared by ultrasound, mechanical agitation, and the handmade Tessari method for treatment of varicose veins. *Journal of Ultrasound in Medicine: Official Journal of the American Institute of Ultrasound in Medicine*, *36*(3), 649–658. https://doi.org/10.7863/ultra.16.02052

Debrégeas, G., Tabuteau, H., & Di Meglio, J. M. (2001). Deformation and flow of a two-dimensional foam under continuous shear. *Physical Review Letters*, *87*(17). https://doi.org/10.1103/PhysRevLett.87.178305

Denkov, N. D., Subramanian, V., Gurovich, D., & Lips, A. (2005). Wall slip and viscous dissipation in sheared foams: Effect of surface mobility. *Colloids and Surfaces A: Physicochemical and Engineering Aspects*, *263*, 129–145. https://doi.org/10.1016/j.colsurfa.2005.02.038

Denkov, N. D., Tcholakova, S., Golemanov, K., Subramanian, V., & Lips, A. (2006). Foam-wall friction: Effect of air volume fraction for tangentially immobile bubble surface. *Colloids and Surfaces A: Physicochemical and Engineering Aspects*, *282–283*, 329–347. https://doi.org/10.1016/j.colsurfa.2006.04.028

Denkov, N. D., Tcholakova, S., Golemanov, K., Ananthapadmanabhan, K. P., & Lips, A. (2008). Viscous friction in foams and concentrated emulsions under steady shear. *Physical Review Letters*, *100*(13). https://doi.org/10.1103/PhysRevLett.100.138301

Denkov, N. D., Tcholakova, S., Golemanov, K., Ananthpadmanabhan, K. P., & Lips, A. (2009). The role of surfactant type and bubble surface mobility in foam rheology. *Soft Matter*, *5*(18), 3389–3408. https://doi.org/10.1039/b903586a

Denn, M. M., & Bonn, D. (2011). Issues in the flow of yield-stress liquids. *Rheologica Acta*, *50*(4), 307–315. https://doi.org/10.1007/s00397-010-0504-3

Dinkgreve, M., Paredes, J., Denn, M. M., & Bonn, D. (2016). On different ways of measuring "the" yield stress. *Journal of Non-Newtonian Fluid Mechanics*, *238*, 233–241. https://doi.org/10.1016/j.jnnfm.2016.11.001

Dollet, B., & Raufaste, C. (2014). Rheology of aqueous foams. *Comptes Rendus Physique*, *15*, 731–747. https://doi.org/10.1016/j.crhy.2014.09.008

Doraiswamy, D., Mujumdar, A. N., Tsao, I., Beris, A. N., Danforth, S. C., & Metzner, A. B. (2002). The Cox–Merz rule extended: A rheological model for concentrated suspensions and other materials with a yield stress. *Journal of Rheology*, *35*(4), 647–685. https://doi.org/10.1122/1.550184

Drapaca, C. (2018). Poiseuille flow of a non-local non-Newtonian fluid with wall slip: A first step in modeling cerebral microaneurysms. *Fractal and Fractional*, *2*(1), 9. https://doi.org/10.3390/fractalfract2010009

Eckmann, D. M. (2009). Polidocanol for endovenous microfoam sclerosant therapy. *Expert Opinion on Investigational Drugs*, *18*, 1919–1927. https://doi.org/10.1517/13543780903376163

Enzendorfer, C., Harris, R. A., Valkó, P., Economides, M. J., Fokker, P. A., & Davies, D. D. (2002). Pipe viscometry of foams. *Journal of Rheology*, *39*(2), 345–358. https://doi.org/10.1122/1.550701

Evans, M. E., Kraynik, A. M., Reinelt, D. A., Mecke, K., & Schröder-Turk, G. E. (2013). Networklike propagation of cell-level stress in sheared random foams. *Physical Review Letters*, *111*(13). https://doi.org/10.1103/PhysRevLett.111.138301

Fiorillo, A. S, Fiorillo, A. S., Critello, D. C., & Pullano, S.. (2015). Acoustic cavitation for producing foam in sclerosant drugs. Paper presented at 2015 AEIT International Annual Conference, AEIT 2015. Retrieved from https://doi.org/10.1109/AEIT.2015.7415276.

Forlee, M. V., Grouden, M., Moore, D. J., & Shanik, G. (2006). Stroke after varicose vein foam injection sclerotherapy. *Journal of Vascular Surgery*, *43*(1), 162–164. https://doi.org/10.1016/j.jvs.2005.09.032

Gardiner, B. S., Dlugogorski, B. Z., & Jameson, G. J. (1998). Rheology of fire-fighting foams. *Fire Safety Journal*, *31*(1), 61–75. https://doi.org/10.1016/S0379-7112(97)00049-0

Geroulakos, G. (2006). Foam sclerotherapy for the management of varicose veins: A critical reappraisal. *Phlebolymphology*, 202–206.

Gibson, K., & Gunderson, K. (2018). Liquid and foam sclerotherapy for spider and varicose veins. *Surgical Clinics of North America*, *98*, 415–429. https://doi.org/10.1016/j.suc.2017.11.010

Gloviczki, P., Comerota, A. J., Dalsing, M. C., Eklof, B. G., Gillespie, D. L., Gloviczki, M. L., … American Venous Forum. (2011). The care of patients with varicose veins and associated chronic venous diseases: Clinical practice guidelines of the Society for Vascular Surgery and the American Venous Forum. *Journal of Vascular Surgery*, *53*(5 Suppl), 2S–48S. https://doi.org/10.1016/j.jvs.2011.01.079

Gopal, A. D., & Durian, D. J. (1999). Shear-induced "melting" of an aqueous foam. *Journal of Colloid and Interface Science*, *213*(1), 169–178. https://doi.org/10.1006/jcis.1999.6123

Guyton, A. C., & Hall, J. E. (2006). Chapter 15: Vascular distensibility and functions of the arterial and venous systems. In *Textbook of medical physiology*.

Hackley, V. A., & Ferraris, C. F. (2001). *NIST recommended practice guide: The use of Nomenclature in Dispersion Science and Technology|NIST*. Special Publication (NIST SP) - 960-3, p. 39.

Hamel-Desnos, C., Desnos, P., Wollmann, J. C., Ouvry, P., Mako, S., & Allaert, F. A. (2003). Evaluation of the efficacy of polidocanol in the form of foam compared with liquid form in sclerotherapy of the greater saphenous vein: Initial results. *Dermatologic Surgery*, *29*(12), 1170–1175. https://doi.org/10.1111/j.1524-4725.2003.29398.x

De Hart, J., Peters, G. W. M., Schreurs, P. J. G., & Baaijens, F. P. T. (2000). A two-dimensional fluid-structure interaction model of the aortic value. *Journal of Biomechanics*, *33*(9), 1079–1088. https://doi.org/10.1016/S0021-9290(00)00068-3

De Hart, J., Peters, G. W. M., Schreurs, P. J. G., & Baaijens, F. P. T. (2003). A three-dimensional computational analysis of fluid-structure interaction in the aortic valve. *Journal of Biomechanics*, *36*(1), 103–112. https://doi.org/10.1016/S0021-9290(02)00244-0

Hashimoto, K., Uchida, B., Horikawa, M., Mimura, H., & Farsad, K. (2018). Effects of different mixing agents on the stability of sodium tetradecyl sulfate (STS) foam: An experimental study. *Cardiovascular and Interventional Radiology*, *41*(12), 1952–1957. https://doi.org/10.1007/s00270-018-2049-2

Hathcock, J. J. (2006). Flow effects on coagulation and thrombosis. *Arteriosclerosis, Thrombosis, and Vascular Biology*, *26*, 1729–1737. https://doi.org/10.1161/01.ATV.0000229658.76797.30

Herzhaft, B. (1999). Rheology of aqueous foams: A literature review of some experimental works. *Oil and Gas Science and Technology*, *54*, 587–596. https://doi.org/10.2516/ogst:1999050

Herzhaft, B., Kakadjian, S., & Moan, M. (2005). Measurement and modeling of the flow behavior of aqueous foams using a recirculating pipe rheometer. *Colloids and Surfaces A: Physicochemical and Engineering Aspects*, *263*, 153–164. https://doi.org/10.1016/j.colsurfa.2005.01.012

Höhler, R., & Cohen-Addad, S. (2005). Rheology of liquid foams. *Journal of Physics: Condensed Matter*, *17*(41), R1041–R1069. https://doi.org/10.1016/0378-4371(94)90221-6

Jang, S. S., & Goddard, W. A. (2006). Structures and properties of newton black films characterized using molecular dynamics simulations. *Journal of Physical Chemistry B*, *110*(15), 7992–8001. https://doi.org/10.1021/jp056685c

Jones, L., Braithwaite, B. D., Selwyn, D., Cooke, S., & Earnshaw, J. J. (1996). Neovascularisation is the principal cause of varicose vein recurrence: Results of a randomised trial of stripping the long saphenous vein. *European Journal of Vascular and Endovascular Surgery*, *12*(4), 442–445. https://doi.org/10.1016/S1078-5884(96)80011-6

Karakashev, S. I. (2017). Hydrodynamics of foams. *Experiments in Fluids*, *58*. https://doi.org/10.1007/s00348-017-2332-z

Katgert, G., Tighe, B. P., & Van Hecke, M. (2013). The jamming perspective on wet foams. *Soft Matter*, *9*, 9739–9746. https://doi.org/10.1039/c3sm51543e

Khan, S. A., & Armstrong, R. C. (1986). Rheology of foams: I. Theory for dry foams. *Journal of Non-Newtonian Fluid Mechanics*, *22*(1), 1–22. https://doi.org/10.1016/0377-0257(86)80001-5

Khan, S. A., & Armstrong, R. C. (1987). Rheology of foams: II. Effects of polydispersity and liquid viscosity for foams having gas fraction approaching unity. *Journal of Non-Newtonian Fluid Mechanics*, *25*(1), 61–92. https://doi.org/10.1016/0377-0257(87)85013-9

Khan, S. A., Schnepper, C. A., & Armstrong, R. C. (1988). Foam rheology: III. Measurement of shear flow properties. *Journal of Rheology*, *32*(1), 69–92. https://doi.org/10.1122/1.549964

Kolluri, R., Hays, K. U., & Gohel, M. S. (2018). Foam sclerotherapy augmented phlebectomy (SAP) procedure for varicose veins: Report of a novel technique. *EJVES Short Reports*, *41*, 16–18. https://doi.org/10.1016/j.ejvssr.2018.10.007

Kraynik, A. (1988). Foam flows. *Annual Review of Fluid Mechanics*, *20*(1), 325–357. https://doi.org/10.1146/annurev.fluid.20.1.325

Kraynik, A. M., Reinelt, D. A., & van Swol, F. (2003). Structure of random monodisperse foam. *Physical Review E—Statistical Physics, Plasmas, Fluids, and Related Interdisciplinary Topics*, *67*(3), 11. https://doi.org/10.1103/PhysRevE.67.031403

Kraynik, A. M., Reinelt, D. A., & Van Swol, F. (2004). Structure of random foam. *Physical Review Letters*, *93*(20). https://doi.org/10.1103/PhysRevLett.93.208301

Kroezen, A. B. J., Wassink, J. G., & Schipper, C. A. C. (1988). The flow properties of foam. *Journal of the Society of Dyers and Colourists*, *104*(10), 393–400. https://doi.org/10.1111/j.1478-4408.1988.tb01138.x

Larmignat, S., Vanderpool, D., Lai, H. K., & Pilon, L. (2008). Rheology of colloidal gas aphrons (microfoams). *Colloids and Surfaces A: Physicochemical and Engineering Aspects*, *322*(1–3), 199–210. https://doi.org/10.1016/j.colsurfa.2008.03.010

Lin, F., Zhang, S., Sun, Y., Ren, S., & Liu, P. (2015). The management of varicose veins. *International Surgery. The International College of Surgeons, World Federation of General Surgeons and Surgical Specialists, Inc*, *100*(1), 185–189. https://doi.org/10.9738/INTSURG-D-14-00084.1

Marsden, G., Perry, M., Bradbury, A., Hickey, N., Kelley, K., Trender, H., … Davies, A. H. (2015). A cost-effectiveness analysis of surgery, endothermal ablation, ultrasound-guided foam sclerotherapy and compression stockings for symptomatic varicose veins. *European Journal of Vascular and Endovascular Surgery*, *50*(6), 794–801. https://doi.org/10.1016/j.ejvs.2015.07.034

Marze, S., Langevin, D., & Saint-Jalmes, A. (2008). Aqueous foam slip and shear regimes determined by rheometry and multiple light scattering. *Journal of Rheology*, *52*(5), 1091–1111. https://doi.org/10.1122/1.2952510

Moneta, G. L. (2012). Air versus physiological gas for ultrasound guided foam sclerotherapy treatment of varicose veins. *Yearbook of Vascular Surgery*, *2012*, 327–328. https://doi.org/10.1016/j.yvas.2011.11.003

Morrison, N., Neuhardt, D. L., Rogers, C. R., McEown, J., Morrison, T., Johnson, E., & Salles-Cunha, S. X. (2008). Comparisons of side effects using air and carbon dioxide foam for endovenous chemical ablation. *Journal of Vascular Surgery*, *47*(4), 830–836. https://doi.org/10.1016/j.jvs.2007.11.020

Mujumdar, A., Beris, A. N., & Metzner, A. B. (2002). Transient phenomena in thixotropic systems. *Journal of Non-Newtonian Fluid Mechanics*, *102*(2), 157–178. https://doi.org/10.1016/S0377-0257(01)00176-8

Musil, D., Herman, J., & Mazuch, J. (2008). Width of the great saphenous vein lumen in the groin and occurrence of significant reflux in the sapheno-femoral junction. *Biomedical Papers of the Medical Faculty of the University Palacký, Olomouc, Czechoslovakia*, *152*(2), 267–270. https://doi.org/10.5507/bp.2008.041

Nanda, S., Mallik, B. B., Das, S., Chatterjee, S. S., Ghosh, S., & Bhattacharya, S. (2017). A study on Bingham plastic characteristics of blood flow through multiple overlapped stenosed arteries. *Saudi Journal of Engineering and Technology*, *2*(9), 349–357. https://doi.org/10.21276/sjeat.2017.2.9.5

Nastasa, V., Samaras, K., Ampatzidis, C., Karapantsios, T. D., Trelles, M. A., Moreno-Moraga, J., … Pascu, M. L. (2015). Properties of polidocanol foam in view of its use in sclerotherapy. *International Journal of Pharmaceutics*, *478*(2), 588–596. https://doi.org/10.1016/j.ijpharm.2014.11.056

Oklu, R., Habito, R., Mayr, M., Deipolyi, A. R., Albadawi, H., Hesketh, R., … Watkins, M. T. (2012). Pathogenesis of varicose veins. *Journal of Vascular and Interventional Radiology*, *23*, 33–39. https://doi.org/10.1016/j.jvir.2011.09.010

de Oliveira, R. G., de Morais-Filho, D., Engelhorn, C. A., Kessler, I., & Neto, F. C. (2018). Foam sclerotherapy for lower-limb varicose veins: Impact on saphenous vein diameter. *Radiologia Brasileira*, *51*(6), 372–376. https://doi.org/10.1590/0100-3984.2017.0184

Osei-Bonsu, K., Shokri, N., & Grassia, P. (2016). Fundamental investigation of foam flow in a liquid-filled Hele-Shaw cell. *Journal of Colloid and Interface Science*, *462*, 288–296. https://doi.org/10.1016/j.jcis.2015.10.017

Parikh, D. (2017). *Experimental study of pressure drop and bubble size in a laboratory scale compressed air foam*. (master's thesis). Colorado School of Mines, Golden, Colorado.

Parsi, K., Exner, T., Connor, D. E., Herbert, A., Ma, D. D. F., & Joseph, J. E. (2008). The lytic effects of detergent sclerosants on erythrocytes, platelets, endothelial cells and microparticles are attenuated by albumin and other plasma components in vitro. *European Journal of Vascular and Endovascular Surgery.*, *36*, 216–223. https://doi.org/10.1016/j.ejvs.2008.03.001

Parsi, K. (2015). Interaction of detergent sclerosants with cell membranes. *Phlebology*, *30*, 306–315. https://doi.org/10.1177/0268355514534648

Princen, H. M. (1983). Rheology of foams and highly concentrated emulsions. I. Elastic properties and yield stress of a cylindrical model system. *Journal of Colloid and Interface Science*, *91*(1), 160–175. https://doi.org/10.1016/0021-9797(83)90323-5

Princen, H. M. (1985). Rheology of foams and highly concentrated emulsions. II. Experimental study of the yield stress and wall effects for concentrated oil-in-water emulsions. *Journal of Colloid and Interface Science*, *105*(1), 150–171. https://doi.org/10.1016/0021-9797(85)90358-3

Princen, H. M., & Kiss, A. D. (1986). Rheology of foams and highly concentrated emulsions. III. Static shear modulus. *Journal of Colloid And Interface Science*, *112*(2), 427–437. https://doi.org/10.1016/0021-9797(86)90111-6

Princen, H. M., & Kiss, A. D. (1989). Rheology of foams and highly concentrated emulsions. IV. An experimental study of the shear viscosity and yield stress of concentrated emulsions. *Journal of Colloid and Interface Science*, *128*(1), 176–187. https://doi.org/10.1016/0021-9797(89)90396-2

Rabe, E., & Pannier, F. (2010). Sclerotherapy of varicose veins with polidocanol based on the guidelines of the german society of phlebology: Original articles. *Dermatologic Surgery*, *36*(SUPPL. 2), 968–975. https://doi.org/10.1111/j.1524-4725.2010.01495.x

Ramadan, W. M., El-Hoshy, K. H., Shaaban, D. M., Hassan, A. M., & El-Sharkawy, M. M. (2011). Clinical comparison of sodium tetradecyl sulfate 0.25% versus polidocanol 0.75% in sclerotherapy of lower extremity telangiectasia. *The Gulf Journal of Dermatology and Venereology*, *18*(2), 33–40.

Raynaud, J. S., Moucheront, P., Baudez, J. C., Bertrand, F., Guilbaud, J. P., & Coussot, P. (2002). Direct determination by nuclear magnetic resonance of the thixotropic and yielding behavior of suspensions. *Journal of Rheology*, *46*(3), 709–732. https://doi.org/10.1122/1.1463420

Recek, C. (2006). Conception of the venous hemodynamics in the lower extremity. *Angiology*, *57*(5), 556–563. https://doi.org/10.1177/0003319706293117

Recek, C. (2013). Calf pump activity influencing venous hemodynamics in the lower extremity. *International Journal of Angiology*, *22*, 23–30. https://doi.org/10.1055/s-0033-1334092

Van Rij, A. M., Jones, G. T., Hill, G. B., & Jiang, P. (2004). Neovascularization and recurrent varicose veins: More histologic and ultrasound evidence. *Journal of Vascular Surgery*, *40*(2), 296–302. https://doi.org/10.1016/j.jvs.2004.04.031

Rouyer, F., Cohen-Addad, S., Vignes-Adler, M., & Höhler, R. (2003). Dynamics of yielding observed in a three-dimensional aqueous dry foam. *Physical Review E - Statistical Physics, Plasmas, Fluids, and Related Interdisciplinary Topics*, *67*(2), 7. https://doi.org/10.1103/PhysRevE.67.021405

Saint-Jalmes, A. (2006). Physical chemistry in foam drainage and coarsening. *Soft Matter*, *2*(10), 836–849. https://doi.org/10.1039/b606780h

Saint-Jalmes, A., & Langevin, D. (2002). Time evolution of aqueous foams: Drainage and coarsening. *Journal of Physics Condensed Matter*, *14*(40 Spec), 9397–9412. https://doi.org/10.1088/0953-8984/14/40/325

Shi, X., Yang, J., Huang, J., Long, Z., Ruan, Z., Xiao, B., & Xi, X. (2016). Effects of different shear rates on the attachment and detachment of platelet thrombi. *Molecular Medicine Reports*, *13*(3), 2447–2456. https://doi.org/10.3892/mmr.2016.4825

Somers, P., & Knaapen, M. (2006). The histopathology of varicose vein disease. *Angiology*, *57*, 546–555. https://doi.org/10.1177/0003319706293115

Song, H. Y., Salehiyan, R., Li, X., Lee, S. H., & Hyun, K. (2017). A comparative study of the effects of cone-plate and parallel-plate geometries on rheological properties under oscillatory shear flow. *Korea Australia Rheology Journal*, *29*(4), 281–294. https://doi.org/10.1007/s13367-017-0028-9

de Souza Mendes, P. R. (2009). Modeling the thixotropic behavior of structured fluids. *Journal of Non-Newtonian Fluid Mechanics*, *164*(1–3), 66–75. https://doi.org/10.1016/j.jnnfm.2009.08.005

Star, P., Connor, D. E., & Parsi, K. (2018). Novel developments in foam sclerotherapy: Focus on Varithena® (polidocanol endovenous microfoam) in the management of varicose veins. *Phlebology*, *33*, 150–162. https://doi.org/10.1177/0268355516687864

Sun, Y., Qi, X., Sun, H., Zhao, H., & Li, Y. (2016). Understanding about how different foaming gases effect the interfacial array behaviors of surfactants and the foam properties. *Langmuir*, *32*(30), 7503–7511. https://doi.org/10.1021/acs.langmuir.6b02269

TA Instruments. (2000). *Rheological techniques for yield stress analysis*. TA Instruments Technical notes - RH025.

Tessari, L. (2002). Method and apparatus for producing an injectable foam. United States.

Tessari, L., Cavezzi, A., & Frullini, A. (2001). Preliminary experience with a new sclerosing foam in the treatment of varicose veins. *Dermatologic Surgery*, *27*(1), 58–60. https://doi.org/10.1046/j.1524-4725.2001.00192.x

Todd, K. L., Wright, D. I., & VANISH-2 Investigator Group. (2014). The VANISH-2 study: A randomized, blinded, multicenter study to evaluate the efficacy and safety of polidocanol endovenous microfoam 0.5% and 1.0% compared with placebo for the treatment of saphenofemoral junction incompetence. *Phlebology*, *29*(9), 608–618. https://doi.org/10.1177/0268355513497709

Tortora, G. J., & Derrickson, B. (2014). The cardiovascular system: Blood vessels and hemodynamics. In *Principles of anatomy & physiology* (14th ed.). Wiley.

Tseng, H., Pilon, L., & Warrier, G. R. (2006). Rheology and convective heat transfer of colloidal gas aphrons in horizontal mini-channels. *International Journal of Heat and Fluid Flow*, *27*(2), 298–310. https://doi.org/10.1016/j.ijheatfluidflow.2005.08.009

Updegrove, A., Wilson, N. M., Merkow, J., Lan, H., Marsden, A. L., & Shadden, S. C. (2017). SimVascular: An open source pipeline for cardiovascular simulation. *Annals of Biomedical Engineering*, *45*, 525–541. https://doi.org/10.1007/s10439-016-1762-8

Valkó, P., & Economides, M. J. (2002). Volume equalized constitutive equations for foamed polymer solutions. *Journal of Rheology*, *36*(6), 1033–1055. https://doi.org/10.1122/1.550300

Vein Centre. (2019). *Varicose vein treatment prices*. Retrieved from https://www.veincentre.com/our-prices/basic-prices/#menu.

Watkins, M. R. (2011). Deactivation of sodium tetradecyl sulphate injection by blood proteins. *European Journal of Vascular and Endovascular Surgery*, *41*(4), 521–525. https://doi.org/10.1016/j.ejvs.2010.12.012

Whiteley, M. S. (2011) *Understanding venous reflux: The cause of varicoses veins and venous leg ulcers*. Whiteley Pub. Limited. Retrieved from http://www.markwhiteley.co.uk/books-mark-whiteley.php.

Wong, K., Chen, T., Connor, D. E., Behnia, M., & Parsi, K. (2015). Basic physiochemical and rheological properties of detergent sclerosants. *Phlebology*, *30*(5), 339–349. https://doi.org/10.1177/0268355514529271

Wong, K. C., Chen, T., Connor, D. E., Behnia, M., & Parsi, K. (2014). Computational fluid dynamics of liquid and foam sclerosant injection in a vein model. *Applied Mechanics and Materials*, *553*, 293–298. https://doi.org/10.4028/www.scientific.net/amm.553.293

Wong, M. (2015). Should foam made with physiologic gases be the standard in sclerotherapy? *Phlebology*, *30*, 580–586. https://doi.org/10.1177/0268355514560275

Xu, J., Wang, Y. F., Chen, A. W., Wang, T., & Liu, S. H. (2016). A modified Tessari method for producing more foam. *Springerplus*, *5*(1), 1–3. https://doi.org/10.1186/s40064-016-1769-5

Yiannakopoulou, E. (2016). Safety concerns for sclerotherapy of telangiectases, reticular and varicose veins. *Pharmacology*, *98*, 62–69. https://doi.org/10.1159/000445436

Zhang, S., & Melander, S. (2014). Varicose veins: Diagnosis, management, and treatment. *The Journal for Nurse Practitioners*, *10*(6), 417–424. https://doi.org/10.1016/j.nurpra.2014.03.004

Zheng, X., Wei, Q., & Zhang, H. (2018). Novel developments in polidocanol sclerotherapy: A review. *Journal of Biosciences and Medicines*, *06*(08), 31–41. https://doi.org/10.4236/jbm.2018.68003

How to cite this article: Meghdadi A, Jones SA, Patel VA, Lewis AL, Millar TM, Carugo D. Foam-in-vein: A review of rheological properties and characterization methods for optimization of sclerosing foams. *J Biomed Mater Res*. 2020; 1–23. https://doi.org/10.1002/jbm.b.34681